UNIVERSITY OF OKLAHOMA

GRADUATE COLLEGE

SHALE CHARACTERIZATION FOR EVALUATING SHALE-DRILLING FLUID INTERACTION

A THESIS

SUBMITTED TO THE GRADUATE FACULTY

in partial fulfillment of the requirements for the

Degree of

MASTER OF SCIENCE

By

KEHINDE ADESOYE
Norman, Oklahoma
2009

SHALE CHARACTERIZATION FOR EVALUATING
SHALE-DRILLING FLUID INTERACTION

A THESIS APPROVED FOR THE
MEWBOURNE SCHOOL OF PETROLEUM AND GEOLOGICAL ENGINEERING

BY

_____
Dr. Samuel Osisanya, Chair

_____
Dr. Subhash Shah

_____
Dr. Ramadan Ahmed

“Intelligence and character are the true goals of education”

Martin Luther King

To God who in his infinite mercy and wisdom ordained my journey through time and brought me to a wonderful place of fulfillment

To my irreplaceable family whom I love with all my heart – Olajide, Folasade, Yetunde, Adebola, Taiwo and Damilola for their prayers, support, and never wavering confidence in my God-given abilities

To my second half, my twin sister, Taiwo Adesoye, you truly are a gem. I could never have come this far without you. You know my most personal struggles and you saw me through them all. I pray that I have been to you, what you have always been to me.
I love you

To my best friend, Chiedozie Ekweribe, for being an instrument in the design and execution of my success, for inspiration when I had none left, and for hope in times of distress
You will be blessed for being a blessing to me

ACKNOWLEDGEMENTS

I would like to thank the chairman of my committee, Dr. Osisanya for his guidance and support during the course of my education. His continual motivation made this study possible. I will never forget his words of wisdom for years to come. I would also like to thank the members of my committee Dr. Shah and Dr. Ahmed for their contributions, suggestions and dedication during the course of my project.

Special thanks to the IC^3 Laboratory of the University of Oklahoma: Dr. Rai, Dr. Sondergeld and their students; for the provision of shale samples and permission to freely use equipment provided in the laboratory. To the WCTC Laboratory and its director Dr. Shah, my thanks for provision of materials for my studies.

I would also like to thank Mr. Mike Shaw and Mr. Gary Stowe for their ideas and assistance during the course of my experimental work.

My huge thanks to the faculty and staff of the Mewbourne School of Petroleum and Geological Engineering for their benevolence and prompt attention to my questions and needs.

Finally, special thanks to all my colleagues friends for their support in everyway. You have all made this a very wonderful experience.

TABLE OF CONTENTS

LIST OF TABLES

LIST OF FIGURES

ABSTRACT

Diminishing oil reserves and increased costs associated with oil and gas recovery have created the need to drill in challenging formations. Shale formations in particular always generated a wide variety of problems when drilled through using conventional water-based muds. Furthermore, the complexity and variations in shales have compounded the task of developing suitable drilling fluids. In light of these problems, the study of shale properties and their interactions with fluids will continue to be a much needed source of information in the oil industry.

This research provides novel information on the characterization of two shale types (Norway and Barnett) and the development of inhibitive water-based muds for the reactive Norway shale. The study includes the determination of shale properties such as mineralogy, cation exchange capacity, native moisture content and total organic carbon content. It also involves the establishment of an adsorption isotherm for both shales and the modeling of these isotherms using the Guggenheim, Anderson and DeBoer model, together with pre-established isotherms of the Pierre, Wellington and Mancos shales.

Bentonitic fluids composed of varying bentonite/salt concentrations and polymeric fluids made up of partially hydrolyzed polyacrylamide (PHPA) viscosified brines were prepared and evaluated for the Norway shale using dispersion tests at ambient (75˚F), 150˚F, and 200˚F. Based on the results of the dispersion tests, promising fluids were selected for the swelling tests.

The Barnett shale exhibited the Type II isotherm common to most shales while the Norway shale showed the Type III isotherm. It was observed from adsorption isotherm models that total organic carbon content, although previously ignored, is a

significant factor in the adsorptive and dispersive behaviors exhibited by shales. Adsorption isotherm model predictions were in agreement with experimental observations for both shales. The Barnett shale exhibited no dispersion after testing with deionized water. It was thus regarded as unreactive and further dispersion and swelling tests were terminated. For the Norway shale, polymeric fluids yielded higher shale percent recovery values from dispersion tests compared to bentonitic fluids. Comparison of PHPA viscosified brine, Xanthan viscosified brine and Methylglucoside/PHPA fluids showed that the Methylglucoside/PHPA fluid gave maximum inhibition for the Norway shale.

CHAPTER 1: INTRODUCTION

1.1 Overview

Interests in the design of water-based muds (WBM) have escalated due to wellbore instability issues that arise from the abundance of problematic shales encountered while drilling. Shales are simply fine-grained sedimentary rocks characterized by low permeability, medium to high clay content, and medium porosity (Oleas et al. 2008). They account for over 75% of formations drilled all over the world and cause over 90% of wellbore instability problems. Wellbore instability is a well established problem which results in substantial yearly expenditure for the drilling industry. Shale types range from soft Gumbo shale in offshore Louisiana, Gulf of Mexico to hard brittle shale in South Louisiana with each type presenting its own set of problems.

Conventional water-based muds (WBMs) that are used to drill through water sensitive shale formations cause a high degree of wellbore instability. Consequently, oil-based muds (OBMs) were adopted to solve the wellbore instability problems due to their superior shale stabilization properties (Patel et al. 2007). Unfortunately, high costs, environmental restrictions, cuttings and used mud disposal difficulties, and safety have largely limited the use of OBMs. All over the world, restrictions on the types of drilling fluids used are continually being evaluated with respect to their environmental compatibility. Consequently, WBMs that have the ability to effectively reduce shale instability problems have once again come under the limelight to replace the OBMs.

The limited availability of models to adequately describe shale fluid interaction has hindered the growth of inhibitive WBM development. Models based on chemical potential and hydraulic pressure developed by Osisanya (1991), Mody and Hale (1993),

Osisanya and Chenevert (1996) and further expanded on by Van Oort et al. (1996) have indicated the complexity of theoretical analysis of driving forces and mechanisms that govern shale stability in the borehole. As a result, the design of such WBMs is mostly experimental. This study investigates and combines various aspects of shale-drilling fluid interactions for the systematic development of WBMs for shale.

1.2 Problem Description

The art and science of drilling wells require the use of drilling fluids for several reasons including cuttings carrying and maintenance of wellbore stability. Drilling fluid selection is dependent on the behavior of the formation to be drilled. Shale, the most abundant rock type in the earth interacts variably with the fluids used. The use of conventional WBMs in drilling shale results in the adsorption of water associated with the drilling mud onto the surface of shale (Chenevert 1970). Depending on the shale type, water adsorption may lead to various reactions such as swelling, cuttings dispersion, and increase in pore pressure (O'Brien and Chenevert 1973) creating wellbore instability to varying degrees.

Common failures that occur from shale instability using conventional WBMs include sloughing, caving, stuck pipe, bit balling and increased torque and drag. These failures can grow into massive expenses due to lost non-productive time. These are further compounded into mud treatment costs, difficulties in running casing and poor cement jobs. Overall, it is imperative that WBMs be formulated and tailored to the type of shale formation encountered.

Shales are known to hydrate due to the hydrophilic nature of the clays present in their molecular structure. In particular, the montmorrillonite clay with a specific surface

area of 800 m^2g^{-1} can adsorb water on many sites leading to severe wellbore instability issues. With the limited knowledge of shale-fluid interactions, water based mud design is predominantly experimental, on a shale by shale basis. The complexity of the deposition and diagenesis process by which shales are formed present endless variations in the shale structure, therefore reestablishing the need for continuous research in this area.

1.3 Literature Review

Several literary works have been published with the intent to clarify the uncertainties surrounding shale-fluid interaction. The works cover a variety of perspectives and are either experimental, field trials, or theoretical (modeling) in nature. The study of shale fluid interactions gained momentum in the seventies after a series of publications by Chenevert revealed the importance of drilling fluid activity in the successful inhibition of shale formations. In his first paper, Chenevert (1970) experimentally tested a wide range of shales expanding the little database of knowledge of shale characteristics. He determined the aqueous activity of the shales by developing adsorption isotherms relating their aqueous activities to their water contents. The isopiestic method, which uses desiccators to create controlled humidity environments, was introduced into shale characterization.

The adsorption isotherms developed for each shale were used to determine their respective adsorptive potential and hydrational tendencies. Chenevert (1970) highlighted the importance of restoring the shales to their natural state of hydration by placing them in relative humidity environments of their native activity. Expansion of unconfined shales (i.e. also known as swelling tests) was measured during immersion in water and a relationship between the observed expansion and the amount of water (weight percent)

adsorbed was established. He discovered that all shales, including hard illitic shales thought to initially be inert, showed some reaction when immersed in water. Furthermore, at equal activities, shales with higher clay contents showed an increased weight percent of water adsorbed. The adsorption also led to the generation of internal stresses which causes spalling, compressive strength reduction, and vertical fracturing.

In his second paper, Chenevert (1970) matched the aqueous chemical potentials of OBMs and the shale they were drilled into. Chemical potentials are thermodynamic properties, which can only be quantified through the measurement of activity at constant temperature. Swelling tests were run with OBMs after adjusting the aqueous activities of the water phase with salts. Balancing the aqueous activity of the OBMs with those of the shales resulted in less swelling. Excess salt addition which lowered OBM activity below that of the shale induced water movement out of the shale. This was observed as a shrinkage effect instead of swelling. Field verifications of the developed OBMs were implemented in West Texas and South Louisiana. The OBMs outperformed conventional WBMs.

The contributions of the adsorption isotherm and shale moisture content to shale characterization established previously soon inspired its application. O'Brien and Chenevert (1973) characterized shales with major laboratory procedures. X-Ray diffraction analyses revealed the shale composition while adsorption isotherms generated showed hydrational tendencies. Various fluids tested using the swelling and dispersion tests showed the supremacy of potassium muds in limiting swelling and instability.

Osisanya (1986), Chenevert and Osisanya (1989) investigated and improved established laboratory techniques in shale studies and their applications at wellsites. The

six major techniques evaluated were swelling, dispersion, cation exchange capacity, capillary suction time, adsorption isotherm tests, and the X-Ray diffraction analysis. Testing equipment required for these tests were adjusted to favor their simple application at wellsite locations. This is necessary as shale problems are time dependent. The more the time spent in studying the shale, diagnosing the problem and developing inhibitive drilling fluids, the higher the severity of wellbore instability that occurs.

Following Chenevert's findings, Osisanya (1991) developed a model for shale fluid interaction and used it to predict swelling pressures developed in shales at elevated temperatures and pressures. During his studies, he evaluated the effectiveness of the adsorption-desorption isotherm phenomena in relation to this system interaction by obtaining total aqueous chemical activity of shale in the same manner as Chenevert (1970). Application of the shale activity obtained from the isotherm to the model equation resulted in adsorptive pressure predictions similar to those observed from his swelling tests. Osisanya (1991), Osisanya and Chenevert (1996) also concluded that shale is a 'leaky' membrane and no longer a semi-permeable membrane as originally proposed by Chenevert (1970)

Hale et al. (1993) investigated the influence of chemical potential, also known as the partial molar free energy, of different shales compared to the chemical potential of the internal water phase of OBMs. The relationship between water content and strength for Pierre and Wellington shales was evaluated as a function of the OBMs aqueous activity. It was observed that lowering the activity of the internal water phase of the OBM reduced the water adsorbed by the shale. The need for a model which accounts for the major driving forces involved in shale-fluid interaction soon became evident. Mody and Hale

(1993) created a borehole stability model coupling the mechanical and chemical aspects of shale fluid interactions. The effective stresses at wellbore and the chemical potential differences were incorporated as driving forces. The model predicts mud weight and salinity required to stabilize shales. Experiments were also run to determine the influence of the differences in chemical potential between the shale pore fluid and drilling fluid on pore pressure.

A special oedometer test cell was designed specifically to simulate in-situ conditions. The shale was saturated initially with a fluid having an activity similar to that of the pore fluid. Overburden stress and wellbore pressures were applied until equilibration was reached. The 'pore fluid' was then displaced by a fluid of lower activity while measuring pore pressure. A reduction in pore pressure was observed when a lower activity fluid was used suggesting water movement out of the shale, altering stresses around the wellbore. Chemical potential difference was again confirmed as a driving force for shale stability.

Al-Awad and Smart (1996) also utilized the adsorption isotherm obtained for native and recompacted shales to find their equilibrium activity and restore them back to their native moisture content. This was followed by experimental investigations with four fluids including distilled water and their effects on these shales. Unconfined linear swelling and dispersion tests were run to evaluate shale-fluid interactions. Van Oort et al. (1996) studied water and ion transfer between shales and drilling fluids for better designs of WBMs. Membrane efficiency, solute coefficient, and pore pressure buildup were measured using pressure transmission tests, osmosis tests, and downhole simulator cell tests (DSC) for various salt solutions. The role of modifying the aqueous activity of the

fluid using salts was once again confirmed. Coupling activity modification with surface active polymers could be used to improve WBM performance as it increases shale membrane selectivity. This strategy however was claimed as invalid for tectonically stressed shales.

Simpson et al. (1995) investigated the effect of several fluids with varying activities on Oligocene shale obtained from the North Sea. X-Ray diffraction analyses and DSC tests were carried out. The balanced activity OBM superseded all the fluids used in pore pressure reduction. A water-based mud prepared using a water soluble inorganic material known as methylglucoside (MEG) was similar in performance to the OBM. The WBM aqueous activity was lowered to that of the shales and a reduction in pore pressure was observed.

Chenevert and Pernot (1998) investigated the development of swelling pressures by resulting from interactions between various water–based fluids in contact with problematic North Sea shales. Experimental swelling tests were run while observing pore pressure increases. Compressive strength tests under simulated downhole conditions were also carried out after contact with the various fluids. It was observed that swelling or shrinkage in the shales were a function of the salt type and ionic concentration. Furthermore, strength reduction was eminent with some of the fluids used. Lowering fluid activity by salt addition provided lower swelling pressures, even to a negative value. The membrane efficiency of the shale was found to depend on chemicals dissolved in the water.

A 3-dimensional model for wellbore stability was developed by Yu et al. (2001) that accounted for thermal stresses in addition to water and ion flux. According to this

work, it was confirmed that aqueous activity of the mud is affected by the ion type and flux. The magnitude of osmotic contributions, being a controversial area, was discovered as subject to solute molecular size, shale permeability and membrane efficiency. This is in agreement with Van Oort et al (1996) observing that polymers, due to their molecular sizes increase membrane selectivity, and consequently, osmotic contributions.

Ewy and Morton (2008) assessed the efficiency of four WBMs with varying activities to reduce pore pressure build up. A device simulating downhole conditions of stresses and overbalanced drilling fluid conditions was used while shale pore pressure, swelling and permeability measurements were taken over time. Results of the study show the presence of two physical phenomena which are osmotic membrane and physical plugging of the pore spaces. All muds used showed less swelling than the base case brine.

1.4 Objectives and Significance of Study

The main objectives of this research are as follows:

1. Present a comprehensive review on fundamentals of shales, adsorption isotherm and water based mud development
2. Characterize shale samples and redefine the use of adsorption isotherms for shale characterization
3. Experimentally investigate the development of a water-based mud for Barnett and Norway shale samples by observing shale-fluid interactions

These objectives were achieved by carrying out the following laboratory experiments:

- Mineralogy analysis and determination of total organic carbon content, native moisture content and cation exchange capacity;
- Adsorption isotherm tests. The adsorption isotherms were modeled using a nonlinear regression-least squares method;
- Dispersion and swelling tests.

1.5 Organization of Thesis

Chapter Two of this study focuses on the fundamentals of shale-fluid interactions. This includes shale properties and wellbore instability issues; the adsorption isotherm theory; and drilling fluid types and inhibitive properties. Chapter Three covers the experimental works. These include total organic content determination, mineralogy analysis, native moisture content and cation exchange capacity determination, adsorption isotherm test, dispersion and swelling tests. The experimental development and evaluation of water-based drilling fluids are also offered. Chapter Four details experimental data, data analysis and discussions. Basic properties of the shale samples such as mineralogy, cation exchange capacity, native moisture content and total organic content are presented. The adsorption isotherms obtained for the shale samples are also shown. The performance of the fluids evaluated based on dispersion and swelling tests are discussed. Finally, Chapter Five presents the summary, conclusions, and recommendations of this study.

CHAPTER 2: FUNDAMENTALS OF SHALE, ADSORPTION ISOTHERMS AND SHALE-DRILLING FLUID INTERACTION

Works on the development of water-based muds for shale formations have been published through out the literature. However, a complete solution to the problem can only begin from the comprehensive breakdown of the fundamental concepts surrounding shale-fluid interaction. Three major areas of review naturally arise from water-base mud development for shale instability issues using the adsorption isotherm concept: *a study on shale rocks (a geologist's perspective), the adsorption isotherm phenomenon (a scientist's perspective), and drilling fluids synopsis (an engineer's perspective)*.

2.1 Shales

Shale is a fine-grained, argillaceous, sedimentary rock with significant clay mineral content. A shale's solid phase is composed of clay minerals and small amounts of other non-clay minerals. Non-clay minerals present in shale are generally considered inert making contributions only to physical properties such as density. Conversely, clay minerals exponentially influence shale reactivity in aqueous solution. Even relatively small quantities of some clays can generate extreme reactions. This is because their colloidal size enables advanced physico-chemical communications between clay particles and the aqueous phase of the drilling fluid. In particular, the montmorillonite (smectite) clay is the most sensitive followed by mixed clays with alternating montmorillonite and illite layers, and illites. Negligible swelling tendencies are exhibited by chlorite and kaolinite clay minerals.

2.1.1 Mineralogy

The mineral content of shale is very important when dealing with wellbore instability. Shale is known to overwhelmingly consist of clay minerals and small amounts of other non-clay minerals such as quartz, feldspar and calcite. Clay minerals are therefore highly studied to comprehend shale behavior. Various methods such as X-Ray Diffraction Analysis, Differential Thermal Analysis and Adsorption Spectra are used to identify and quantify the clay minerals present in shales.

Clays are composed of tiny crystal layers called platelets. Platelets possess two basic structures which are tetrahedral and octahedral in shape. The tetrahedral structure consists of a central silicon atom surrounded by oxygen atoms or hydroxyl groups. The octahedral structure on the other hand consists of aluminum or magnesium atoms bound to oxygen atoms or hydroxyl groups. These unit structures form a configuration called sheets when tetrahedron and octahedron units bond with other tetrahedron and octahedron units respectively. Figures 2.1 and 2.2 show the tetrahedron and octahedron unit structures, and also includes the sheet structure of both units.

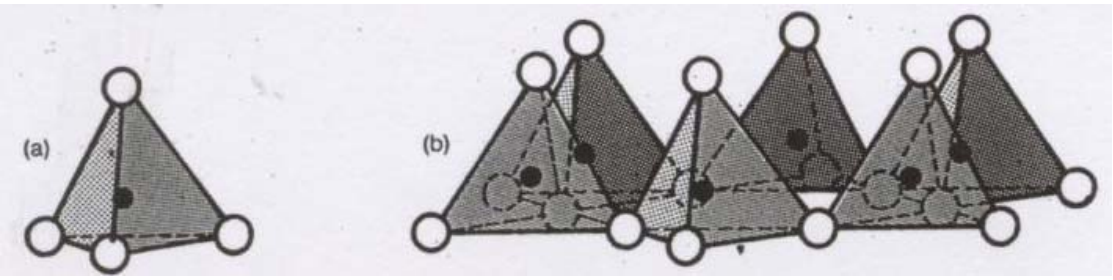

Figure 2.1: a) Single Tetrahedron Unit and b) Sheet Structure for Tetrahedron Units
(After Mitchell 1993)

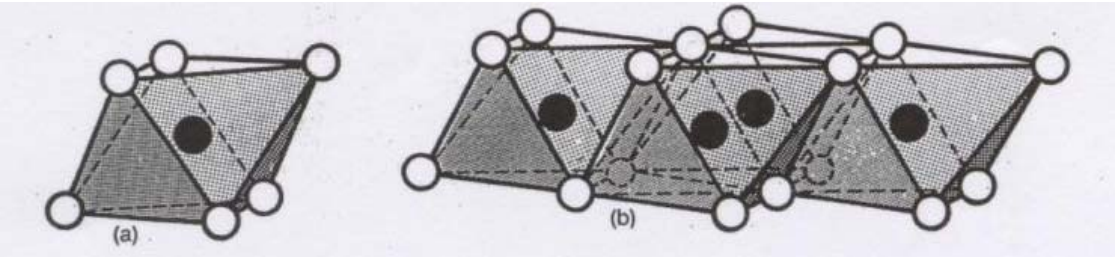

Figure 2.2: a) Single Octahedral Unit and b) Sheet Structure for Octahedral Units (After Mitchell 1993)

Both the tetrahedral and octahedral sheets can be arranged in two primary forms to create a crystal lattice. These include alternating layers of each (1:1) or an octahedral layer sandwiched between two tetrahedral sheets (2:1). Figures 2.3 and 2.4 show both layering types respectively. In the 1:1 configuration, strong covalent bonds exist between the atoms in each unit structure and sheet, leaving little room for lattice substitution. Moreover, strong hydrogen bonds exist between consecutive layers eliminating swelling tendencies. Therefore, shales possessing this configuration are not very reactive e.g. kaolinite. In the 2:1 ratio, only weak Van Der Waal forces hold the adjacent layers together giving more room for expansion when in aqueous solution. In particular, the montmorillonite clay from the smectite group entertains ionic substitution in the octahedral layer. This places a charge deficit in the middle of the unit structure. Associated cations of the structure therefore are not able to balance the charge due to the distance of separation. Adsorption of polar molecules between the sheets is now feasible due to the charge imbalance observed. Figures 2.5 and 2.6 show the structures of montmorillonite-bentonite and kaolinite clay minerals respectively.

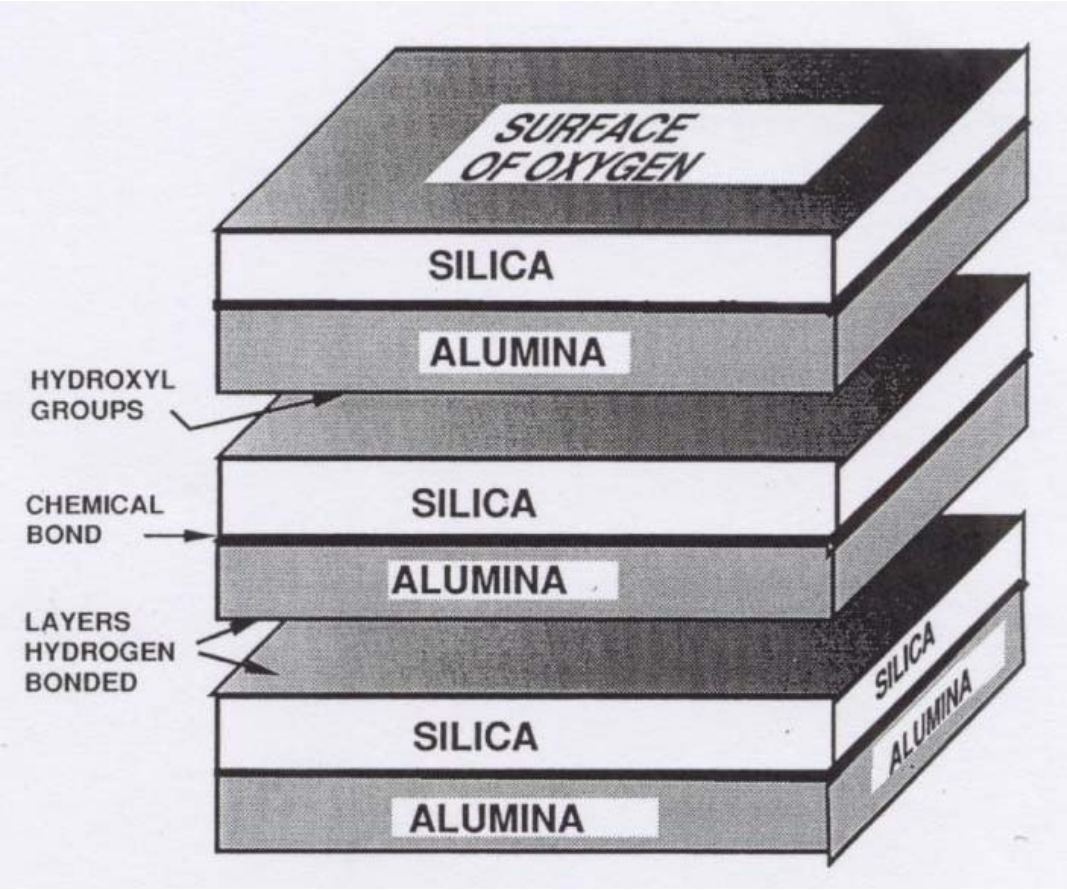

Figure 2.3: A 1:1 Layering Configuration
(After Schechter 1990)

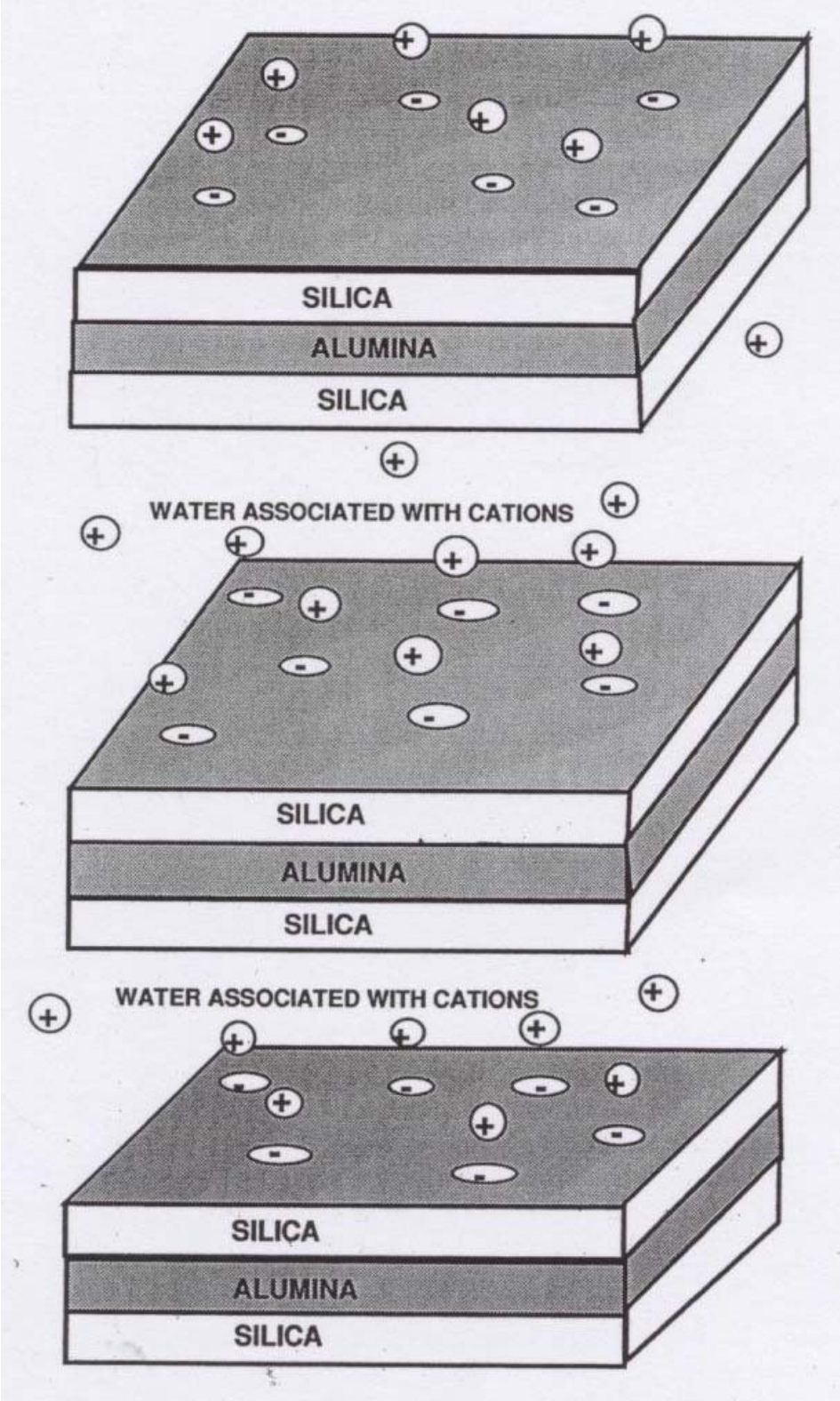

Figure 2.4: A 2:1 Layering Configuration
(After Schechter 1990)

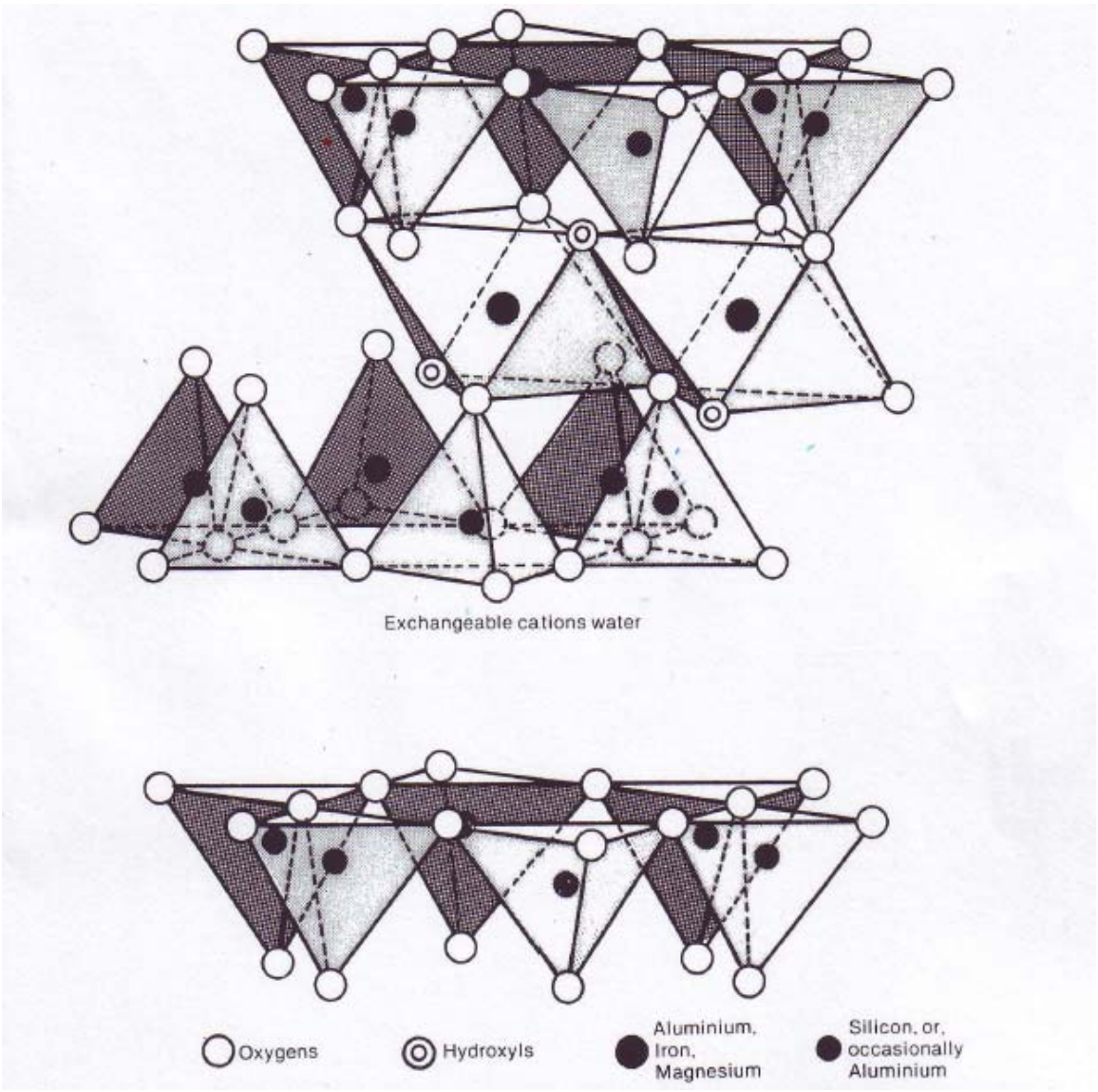

Figure 2.5: Structure of Montmorillonite-Bentonite
(After Mitchell 1993)

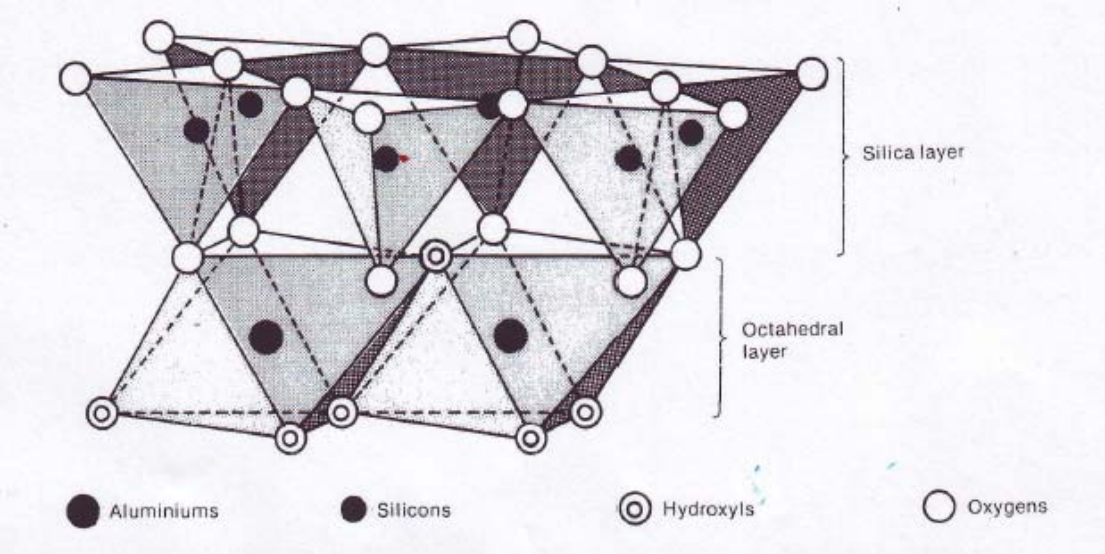

Figure 2.6: Structure of Kaolin
(After Mitchell 1993)

2.1.2 Cation Exchange Capacity

Atoms other than silicon, aluminum and magnesium atoms could be encountered in clay's crystal lattice due to a process known as isomorphous substitution. This is the replacement of an atom by other atoms of similar sizes but lower charges without altering the general structure of the crystal lattice. For example, in the tetrahedral sheet, Si^{4+} may be replaced with Al^{3+} or Fe^{3+}, and in the octahedral sheet Al^{3+} may be replaced by Mg^{2+} and Fe^{2+}. An overall charge deficit now exists causing a negative potential at the clay surface. The clay is now cation-seeking and will readily adsorb a cation to adjust this charge imbalance.

The occurrence of isomorphous substitution and the subsequent adsorption of a cation in clays causes a disparity in their stability. The adsorbed cation is held loosely by the crystal structure and can readily be exchanged for another cation, thus the term cation exchange capacity (CEC). In the presence of water, the cations voluntarily undergo substitution by hydrogen or hydronium ions present. This results in a high affinity for

water molecules which can cause alteration of the shale's physical properties. CEC can be measured in the laboratory by introducing cationic species such as ammonium (NH_4^+), K^+, Na^+, and methylene blue to completely balance the charge deficiency in the clay. The methylene blue test is the simplest and most common test used in the drilling industry. The test results are reported in units of meq/100g (milliequivalent weights of methylene blue/100g of dry clay). The CEC of common clay minerals have been measured and are presented in Table 2.1.

Table 2.1: CEC of Major Clay Minerals (After Boulding and Ginn 2003)

Clay Mineral	CEC (Meq/100g)
Smectite (Montmorillonite)	80 - 150
Chlorites	10 - 40*
Illites	10 - 40*
Kaolinites	3 - 15*

***Upper range occurs with smaller particle size**

2.1.3 Native Moisture Content

Native moisture content is the amount of water present in shale as received in the laboratory after the removal of coatings for preservation. It is unique to each type of shale and the environment in which it is located. In order to accurately obtain the native moisture content of a shale rock, preservation by careful coring and immediate immersion in mineral oil is used to prevent dehydration. Native moisture content in combination with the adsorption isotherm is usually used to obtain the native relative vapor pressure (P/P_o) of shale. Relative vapor pressure is the percent relative humidity divided by 100. It is usually used interchangeably with aqueous activity due to their approximately equal values. A shale's native relative vapor pressure directly corresponds to its adsorptive potential and state of hydration at the native moisture content value.

2.1.4 Aqueous (Water) Activity

Aqueous activity is a fundamental property of shale which directly indicates its state of hydration and its ability to adsorb moisture. It is associated with the water contained in the shale structure and is highly dependent on temperature. In-situ or laboratory measurements of aqueous activity of shales are impossible. Instead, they are determined by measuring relative vapor pressures in the laboratory. A shale's relative vapor pressure is approximately equal to its aqueous activity. This relationship is expressed as follows:

$$a_w \approx \frac{p_w}{p_w^o} \qquad \text{..... (2.1)}$$

where,

$a_w = aqueous\ activity$

$p_w = vapor\ pressure\ of\ water\ in\ shale\ located\ between\ clay\ platelets\ at\ a\ temperature$

$p_w^o = vapor\ pressure\ of\ pure\ water\ at\ the\ same\ temperature$

An important behavior observed in shales is the effect of lowering the aqueous activities of the fluid they are immersed in. Water moves from an environment of higher activity to that of a lower activity. Thus the water moves out of the shale. This gives rise to an increase in potential between the clay platelets, consequently reducing their swelling capability. Another fundamental use of aqueous activity in shale studies is in the determination of adsorptive and swelling pressures realized in shales. An established relationship between these properties is as follows:

$$P_\pi = -P_{ads} = \frac{RT}{V_w}\ln(a_w) \quad \text{.....} \quad (2.2)$$

where,

P_π = *swelling pressure*

P_{ads} = *adsorptive pressure*

R = *universal gas constant*

T = *absolute temperature*

V_w = *partial molar volume*

Vapor pressure above shale water (p_w) is less than the vapor pressure above pure water (p_w^o) due to the fewer number of water molecules present per unit volume of shale. Therefore, the relative vapor pressure of shale water is always less than one. Adsorptive pressures are therefore always negative. Adsorptive pressure values are highly dependent on clay and water content.

2.1.5 Wellbore Instability Issues

Shales are studied due to the wellbore instability challenges that arise when drilling through them. Shales, being highly compacted clay for millions of years become dehydrated (Van 1963) and will immediately adsorb water when in contact with an aqueous solution. The reaction between the shale formation and water in the mud creates instability in the wellbore which can manifest itself in several ways depending on the shale's clay content. O'Brien and Chenevert (1973) classified problematic shales based on their clay content and observed drilling characteristics such as hardness, dispersion,

sloughing and caving tendencies. Table 2.2 shows the classification according to O'Brien and Chenevert (1973).

Table 2.2: Classification of Problem Shales (After O'Brien and Chenevert 1973)

Class	Clay Content	Drilling Characteristics
1	High Montmorillonite Some Illite	Soft, high dispersion
2	Fairly high in montmorillonite High in illite	Soft, fairly high dispersion
3	High in interlayered clays High in illite and chlorite	Medium-hard, moderate dispersion, Sloughing tendencies
4	Moderate illite and chlorite	Hard, little dispersion Sloughing tendencies
5	High in illite, moderate chlorite	Very hard, brittle, no significant dispersion Caving tendencies

They also highlighted three major factors known to cause shale problems; shale swelling, shale cutting dispersion, and abnormal pressure. When not properly managed, these factors further result in borehole washout, bit balling, caving, sloughing and heaving, stuck pipe, high torque and drag among others (Chenevert 1970, Steiger and Leung 1992). The categorization assists in the prediction of down-hole instability conditions and in the selection of drilling fluids to effectively inhibit wellbore instability. However, shale-fluid interactions are dependent on a variety of factors which cannot simply be classified into a few categories. The effect of other factors such as wellbore pressure, temperature, and overburden stress were not considered. Also, shales may fit into one class depending on their clay content and another class based on their drilling characteristics. Additionally, drilling characteristics detected are subject to the observer's interpretation. Moreover, procedures for clay content analysis vary between laboratories causing a disparity in reported values, also making a rigid classification scheme impossible.

Swelling

While drilling through shale formations, there is a movement of drilling fluid filtrate into the formation, which gives rise to swelling. In the case of swelling, the shale formation extends into the wellbore and is eroded by the circulating drilling fluid. Over time, the erosive action expands the hole diameter leading to an enlarged bore hole. *Borehole washout* is the technical term used to describe this occurrence.

Previously, recompacted shale cuttings were used to measure shale swelling due to unavailable coring equipment for obtaining native shale core samples. However, recent advances in the drilling industry have enabled the direct measurement of shale swelling. This progress is particularly important because of the preserved shale properties which make analysis more representative of in-situ conditions. Chenevert (1970) was the pioneer of shale swelling measurements in the laboratory. A strain-gauge transducer and a direct-reading digimatic swelling indicator were used to measure swelling with respect to time. Adsorptive pressures which cause swelling in shales can be predicted using a combination of swell-time and adsorption data.

Cuttings Dispersion

Shale dispersion is a phenomenon that occurs when shale cuttings come in contact with aqueous fluids. While drilling, shale sloughs into the wellbore due to destabilization resulting from reaction with the drilling fluid. This sloughing shale is then dispersed into the fluid. It is important to note that shale dispersion is different from swelling and should therefore be investigated separately. The immediate consequence of shale dispersion is an excessive accumulation of low density solids in the drilling fluid, thereby changing the fluid's properties. Uncontrolled dispersion causes *bit balling* which is the accumulation

of shale on the drill bit. Easily hydratable clay e.g. gumbo, will form a paste-like mixture when in contact with an aqueous fluid and veil the bit teeth from the reappearing formation. Figure 2.7 shows an example of bit balling. The effects of bit balling include reduced ROP and time expended in cleaning or changing the bit. Moreover, mud properties, elevated circulation pressures and extended hole cleaning periods will eventually lead to borehole washouts.

Figure 2.7: Bitballing While Drilling Through Easily Hydratable Shale (Sun Drilling Products Corp. 2009)

2.2 Adsorption

Adsorption is a widely studied phenomenon due to its importance in reactions at material interfaces. Its extension into the drilling industry for the development of inhibitive drilling fluids for shale formations has also motivated research in this area. Several authors, including Mondshine (1969) and Chenevert (1970) have successfully used this concept in the formulation of drilling fluids for shale inhibition.

2.2.1 Theory

Adsorption has being used to describe gas-liquid, gas-solid and liquid-solid surface interactions. During adsorption, the molecules of the gas or liquid form a condensed layer on the liquid or solid surface. The adsorbate (the attached molecules) remain on the adsorbent (the surface) until they are removed through a process called desorption or further react to form another specie.

Various classes of adsorption have been proposed. These include monolayer and multilayer adsorption, physisorption and chemisorption adsorption. However, monolayer and multilayer adsorption are most significant for this study. In monolayer adsorption, only one layer of adsorbate forms on the adsorbent surface while in multilayer, several layers of adsorbates are formed. Figure 2.8 illustrates this classification. As the number of layers increases, the bond strength between each adsorbate layer and the adsorbent surface decreases. Pore condensation is dominant in multilayer adsorption whereas direct adsorbate surface binding is prevalent in monolayer adsorption.

Figure 2.8: Monolayer and Multilayer Adsorption

Clay surfaces possess a natural negative charge which permits the adsorption of cations. Particularly, their layered structure provides ample surface area for adsorption. Moisture adsorbed is not limited to the surface layer, that is, multiple layers of adsorption may also occur. The magnitude of multiple layers formed is dependent on the strength of the Van Der Waals forces on the clay surface and the nature of the moisture adsorbed. Due to the hydrophilic nature of clay minerals, shales having high clay contents have an increased adsorptive tendency for moisture. Therefore, a shale's mineral composition is vital information in the prediction of its adsorptive tendencies.

2.2.2 Adsorption Isotherms

Adsorption is described by the quantity of adsorbate that undergoes adsorption onto a surface. Pertaining to shale-drilling fluid interaction, it is the amount of moisture adsorbed onto the surface of shales. This relationship is conveniently expressed on an adsorption isotherm. Adsorption isotherms are basically plots showing the amount of moisture that adsorbs onto a shale's surface as a function of the relative vapor pressure at constant temperature. Figure 2.9 shows an example of a typical shale adsorption isotherm obtained by Chenevert (1970). Adsorption isotherm profiles are unique to each shale type. This distinctiveness has been attributed to monolayer adsorption, multilayer adsorption and capillary condensation (Baver 1956, Hiemenz 1977, Adamson 1982). The effect of particle size has also been explored by Osisanya (1991) and found to play some role in adsorption isotherm profiles.

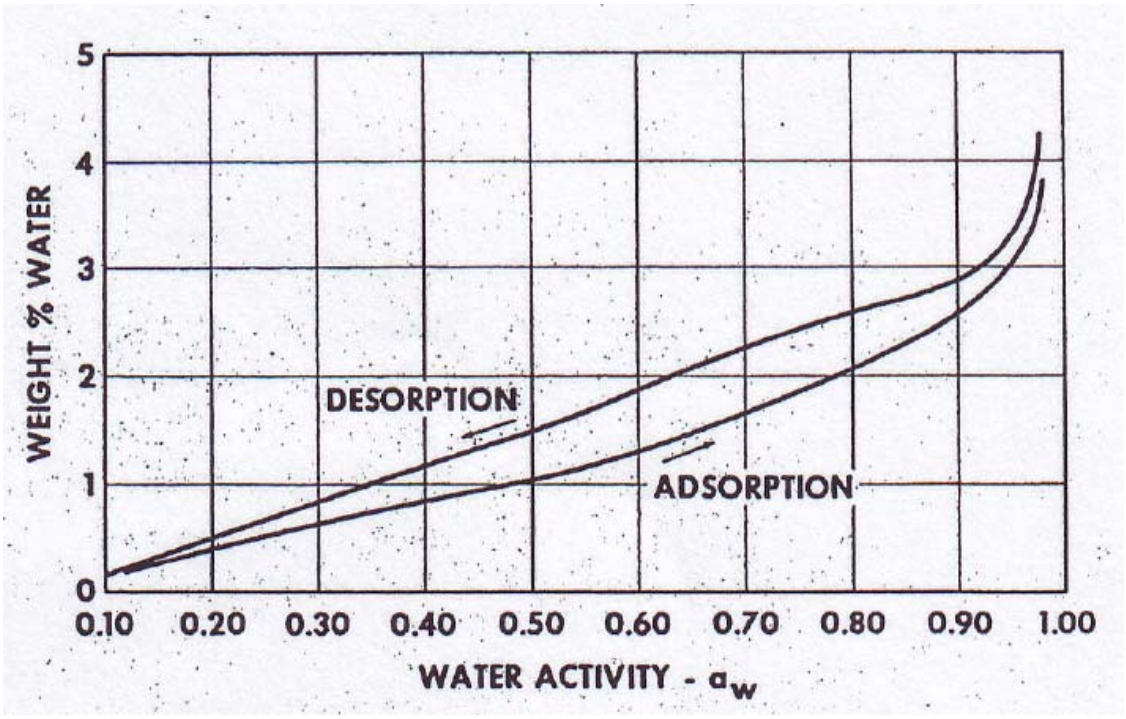

Figure 2.9: Adsorption Isotherm, West Texas Hard Shale (After Chenevert 1970)

Nevertheless, a general trend is still observed in all adsorption isotherms. Overall, there is an increase in adsorbed molecules with increasing pressure, also showing distinct patterns present. The trends observed in adsorption experiments over the years yielded adsorption isotherms that can be categorized into five different types described by Brunauer (1945) and a sixth added by the International Union of Pure and Applied Chemistry (IUPAC) (Figure 2.10). Type I isotherms, also called Langmuir isotherms, exhibit an increasing adsorbate concentration with an increase in pressure until a limiting adsorption is observed. This is usually interpreted as the attainment of a complete monolayer. In type II isotherms, the adsorbate concentration increases with increasing pressures as in type I. However, at higher pressures additional adsorption is observed, this indicates the presence of multiple layers of adsorbent. Type III isotherms describes a case

where minute adsorption is observed initially, followed by a rapid increase in adsorption due to the interaction between subsequent adsorbed layers. Type IV and V are usually observed in porous solids. At the filling of the pores, adsorption is no longer detected. Type VI isotherms show multiple layers of the previous isotherms.

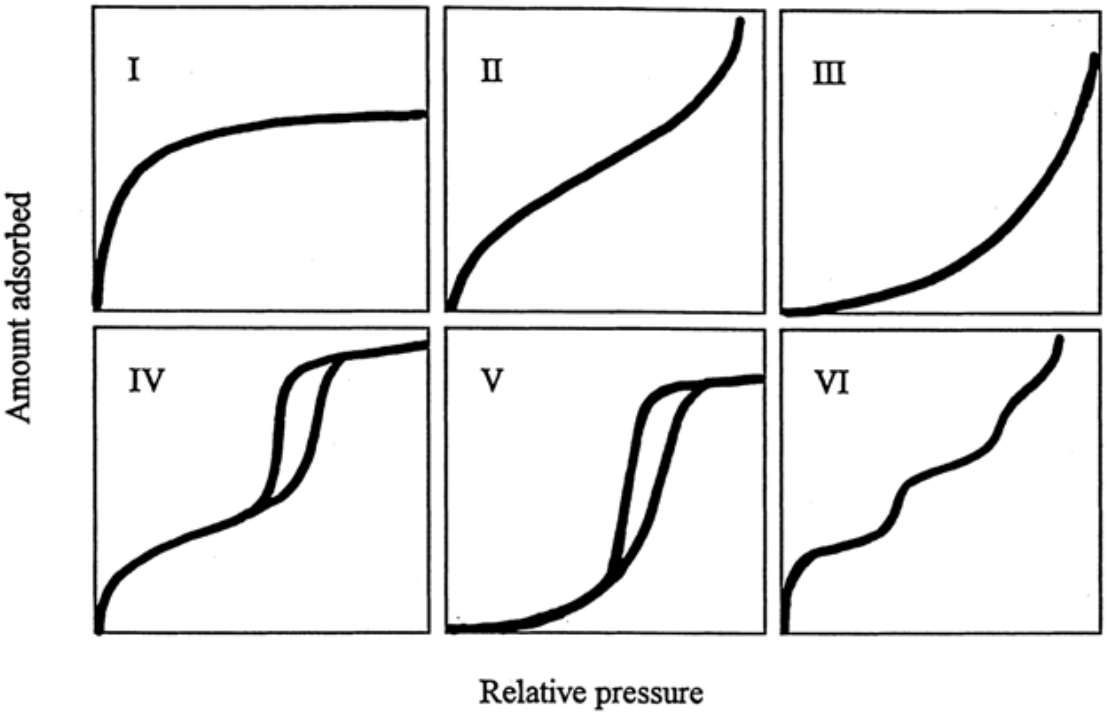

Figure 2.10: IUPAC Classification of Adsorption Isotherms for Gas-Solid Equilibria (After Donohue 1998)

The measurement of shale adsorption isotherms typically involves drying the sample to a constant weight and preserving it in a controlled humidity atmosphere until weight changes are no longer observed. At a constant temperature, the adsorption isotherm obtained can be used to determine information about the shale. These include its primary response to hydration, reactive potential, and consequence of clay quantity on hydration properties (Chenevert 1970, Osisanya 1991).

2.2.3 Analytical Models of Adsorption Isotherms

Several models taking into account monolayer and multilayer adsorption have been described in various literature. The Langmuir adsorption isotherm proposed by Langmuir (1918) is the simplest and one of the most popular isotherm models used to describe the adsorption phenomena. It assumes monolayer adsorption, an interaction between the adsorbate and adsorbent only. The solution of several equilibrium equations led to the development of the Langmuir isotherm expressed in Equation 2.3. The model is limited due to the heterogeneous nature of the adsorbent surface and the adsorbate-adsorbate interactions that occur during the process.

$$\theta(p) = \frac{KP}{1 + KP} \qquad \text{..... (2.3)}$$

where,

θ = *fraction of available active sites*

P = *pressure*

K = *temperature dependent constant*

Due to the limitations of the Langmuir adsorption isotherm, other models were developed to satisfy the need for accuracy and applicability. Over seventy-seven correlations have been proposed for the mathematical interpretation of extensive experimental data as summarized by Van Den Berg and Bruin (1981). Of all these models, the most commonly used are the BET and GAB models in the studies of porous materials (Tsiapouris and Linke 2000).

Developed by Brunauer, Emmett, and Teller, the equation that described the BET adsorption isotherm model was first published in 1938 (Brunauer et al 1938). Improving the Langmuir isotherm, BET developed a model for multiple adsorbed layers. This is particularly favorable in the case of porous materials where multilayer adsorption is most common. In this type of adsorption, interactions are mainly governed by the adsorbate-adsorbate interface. The equation is written as follows in pressure and activity form:

$$v = \frac{v_m cp}{(p_o - p)\{1 + (c-1)(p/p_o)\}} \quad \text{..... (2.4)}$$

$$v = \frac{v_m c a_w}{(1 - a_w)\{1 + (c-1)(a_w)\}} \quad \text{..... (2.5)}$$

where,

v = *moisture content*

v_m = *monolayer moisture content*

p = *pressure*

p_o = *gas saturation pressure*

a_w = *aqueous activity*

c = *constant*

The isotherm has certain advantages and disadvantages which have been identified over the years. The BET model is the only two-parameter model that explains multilayer adsorption (Masel 1996). It fits low activity data extremely well while estimating the amount of adsorbate needed for monolayer coverage, surface area for porous solids, and heat of adsorption. Unfortunately, the model does not fit data above an activity of 0.45 (Wang and Padua 2004).

The Guggenheim, Anderson and DeBoer (GAB) model (Singh and Singh 1996) is a three parameter model developed to further describe adsorption in greater detail. The equation is written in vapor pressure and activity form as shown in Equations 2.5 and 2.6 (Singh and Singh 1996).

$$v = \frac{v_m cKp}{(p_o - Kp)\{1 + (c-1)(Kp/p_o)\}} \quad \text{..... (2.5)}$$

$$v = \frac{v_m cKa_w}{(1 - Ka_w)\{1 + (c-1)(Ka_w)\}} \quad \text{..... (2.6)}$$

where,

v = *moisture content*

v_m = *monolayer moisture content*

p = *pressure*

p_o = *gas saturation pressure*

a_w = *aqueous activity*

c = *guggenheim constant*

K = *sorption energies of the multiple layers of molecules*

The flexibility of the GAB isotherm has been attested through various literatures (McMinn and Magee 1999). It fits over a wide range of activities as used in the food industry (Singh and Singh 1996) and is recommended for describing moisture adsorption onto solid surfaces (Wang and Padua 1994). Therefore, it was used in this study to model the adsorption isotherms obtained.

2.3 Drilling Fluids

"Drilling Fluids" describes a broad range of fluids, both liquids and gases, used in drilling operations to achieve specific purposes. Drilling fluids can generally be classified as water-base fluids, oil-based fluids and gaseous-based fluids. The water-based fluids are used more extensively than the other two due to the advantages they provide. As such more, attention is paid to their development.

2.3.1 Water-Based Fluids

Water is the basic component of most drilling fluids. Water-based fluids are ones in which water is the continuous phase. The performances of water-base fluid is directly related to their density, viscosity, gel strength, and filtration characteristics, and these follow from the colloidal clay fraction of the fluid. Water-based fluids can further be classified into several other types.

1. **Fresh water fluids:** These muds are usually prepared with fresh water and suitable amounts of bentonite or commercial clays. This fluid undergoes little or no chemical treatment before use. An increased rate of penetration is obtained using this mud in inert formations. Examples are spud mud and the natural mud (mud formed when natural water mixes with clay materials in the drilled solids).
2. **Chemically treated mud:** In these muds, chemicals are added to control certain fluid properties such as viscosity which have being altered by the presence of ions encountered while drilling. Chemical reactions take place to remove the unfavorable ions. No calcium compounds are added. Examples are (a) Phosphate fluids, (b) organic treated fluids such as lignite, quebracho and chrome lignosulfonate fluids.

3. **Inhibitive water-based fluids:** An inhibitive water-based fluid is one in which the ability of the active clays to hydrate has been reduced greatly. It is often used to minimize hole sloughing and other "shale" problems. These fluids prevent formation solids from readily disintegrating into extremely fine particles. Commonly used water-based inhibitive fluids are calcium treated fluids (lime muds, $CaCl_2$ and Gypsum ($CaSO_4$) muds; lignosulfonate treated fluids; KCl-polymer, high-salinity fluids (i.e. salt water-based fluids in which sea water or saturated salt water are used as the continuous phase); and oil-emulsion fluids (oil-in-water, i.e. water is the continuous phase).

2.3.2 Oil-Based Fluids

These are fluids in which oil is the continuous liquid phase, diesel oil being the most commonly used. Oil-based fluids can be classify as oil-based or invert emulsion (i.e. water-in-oil) fluids. The basic components are mineral oil, water, emulsifier, wettability reversal agent, viscosity, filtration, alkalinity, and density control agents. The experimental work in this thesis does not involve oil-based fluids, but water-based fluids.

2.3.3 Water-Based Mud and Synthetic-Based Fluids for Shale Inhibition

Several salts, polymers and their combinations (Patel et al. 2007) are among the earliest mud systems recommended for the inhibition of shale swelling. Salts become ions in aqueous solution and are free to move into the clay structure. Here, they occupy spaces which would otherwise be engaged by hydrogen ions from water molecules. The potassium ion in particular is able to inhibit shale reactivity due to its ionic size. This is mainly because the ionic size of the potassium ion, 2.66 Å is closer to that of the space

between the clay platelets, 2.8 Å than any other exchangeable cation (O'Brien and Chenevert 1973).

Polymers are used as viscosifiers in place of bentonite. They assist in improving drilling fluid rheology especially when salts are added. They however do not have the ability to significantly prevent shale failure when used solely (O'Brien and Chenevert 1973). In aqueous solution, the polymer ions and associated molecules react with the water molecules (Hale and Mody 1993) and become hydrated. This process creates a surface area and volume that is higher than dry polymers enabling it to encapsulate or partially coat the shale particles (Clark et al 1976). This layer of adsorbed polymer delays the interaction of water molecules with the shale surface. Examples of polymers include Partially Hydrolyzed Polyacrylamide (PHPA), Xanthan Gum and Carboxy Methyl Cellulose (CMC).

Synthetic materials for mud formulation are novel in the petroleum industry. They represent a cross between OBMs and WBMs, possessing the favorable characteristics of each mud type. SBMs are less reactive to water-sensitive formations and are less toxic to the environment. They are made from synthetic organic based fluids and are evaluated based on their toxicity, biodegradability, thermal stability, viscosity and cost (Patel et al 2007). Example of SBM's include Methylglucoside (MEG), Esters, Ethers, and Polyalphaolefins.

CHAPTER 3: EXPERIMENTAL STUDIES

This chapter consists of two major experiments. These are *shale characterization* and *shale-drilling fluid interaction* experiments. Characterization tests provide knowledge on the composition and properties of the shale while the shale-drilling fluid interaction tests give information on the shale's reactivity in various fluids through dispersion and swelling tests.

The experimental studies involve the following:

1. Characterization of shale samples through mineralogy, total organic content, native moisture content, and cation exchange capacity
2. Development of adsorption isotherms for the shale samples
3. Development and evaluation of various water-based fluid against shale samples
    a. Performing dispersion tests under atmospheric conditions and elevated temperatures of 150˚F and 200˚F
    b. Performing swelling tests under atmospheric conditions

3.1 Shale Test Sample Characterization

Two shale samples were used for this study. The first sample from the Barnett shale play was cored at a depth of 6627.5 ft - 6629.3 ft. It was transported in plastic polythene bags and stored in cardboard boxes. The second sample was obtained from Norway and was cored at a depth of 7072 ft - 7075 ft. This sample was cored and preserved using the oil-based mud used to drill the well and subsequently transferred into

mineral oil before use. The two shale samples were characterized using the following methods:

1. Total organic carbon content – Low Temperature Asher
2. Mineralogy analysis – Fourier Transform InfraRed Spectrometer
3. Native moisture content – Oven
4. Cation exchange capacity – Methylene blue test

3.1.1 Total Organic Carbon (TOC) Content Determination

TOC content is the quantity of carbon associated with organic matter. Organic matter is formed from decaying vegetation and other metabolic activities of living organisms. Shale, being a sedimentary rock formed partly from the deposition of organic material, has organic matter present within its structure. TOC content can be determined using various methods such as high temperature combustion, photo-oxidation, and high temperature catalytic oxidation. The main principle utilized by these methods is the oxidation reaction to remove carbon. For this study, a low temperature asher was used to determine the TOC content.

The shale samples were prepared by grinding them to fine powder of less than 0.01mm using a mallet, mortar and pestle. All instruments were cleaned with acetone to remove any trace amounts of previous shale samples. After grinding, the shales were placed in an oven at 60˚C (140˚F) for 24 hours to remove moisture present in the shale. A layer of the dried shale powder was placed in pre-weighed crucibles and the weight of the shale recorded. It is essential that only one layer of shale is present in order to enable total removal of carbon from the shale. The crucibles were placed in the low temperature asher and a continuous vacuum generated. The low temperature asher sustains an oxygen

plasma at low temperatures within an enclosed chamber while oxidizing the carbon present into carbon dioxide (CO_2). The temperature is low in order to prevent mineral grains from fusing together and distorting the mineral composition of the shale. After ashing for 19 hours, the crucibles were removed and reweighed. The weight of the total organic carbon removed was calculated by taking the difference of the shale weights before and after ashing. The total organic content was calculated as follows:

$$TOC\ (wt\%) = \frac{W_c}{W_s} \times 100 \qquad \text{..... (3.1)}$$

where,

$TOC = total\ organic\ carbon\ (\%)$

$W_c = weight\ of\ carbon\ removed\ by\ ashing\ (g)$

$W_s = weight\ of\ shale\ sample\ before\ ashing\ (g)$

3.1.2 Mineralogy Analysis

Shale mineralogy analysis is used to identify the type and relative amounts of minerals present in shale samples. X-Ray diffraction analysis (XRD) and Fourier Transform Infra Red Spectrometry are common techniques of analysis utilized. According to studies done by Jenkins and Walker (1978), the XRD technique is the best technique for identification while infrared spectrometry is the best for quantitative determination of the minerals. However results from both techniques are highly dependent on particle size and the orientation of the minerals present in the samples. For this study, the Fourier Transform Infra Red Spectrometer (FTIR) was used. The FTIR uses the concept of molecular vibration resulting from radiation to identify the chemical

bonds unique to each compound. The test samples must be carefully prepared by using extremely clean devices, thus eliminating contamination. The results of the FTIR technique are affected by contaminants. The shale samples obtained from the TOC content determination were used for the mineralogy analysis. The removal of organic matter is required because the absorption spectra of organic compounds are more complex than those of inorganic compounds and will take longer to quantify. Moreover, the spectra of the organic compounds were not needed for this study. Further degradation of the shale sample to a 5μm or less sample size was carried out by dissolving the powder in acetone and grinding until the paste dried. A precise 0.5 mg sample of the shale was then dispersed in 0.3 g of potassium bromide (KBr) and pelletized into a small disk. The KBr serves as a background spectrum for the shale sample.

The Norway shale having being immersed in oil required special cleaning before undergoing regular sample preparation. This is because the presence of hydrocarbons will generate similar consequences as that of organic carbon. A soxhlet extraction apparatus was used to remove the oil from the shale sample using toluene as the solvent. Other solvents, e.g. xylene, methanol, or acetone can be used for this process with none having more superiority than others (Civan 2007).

Shale samples were analyzed using a Thermo Nicolet Avatar 370 Furrier Transform InfraRed Spectrometer (FTIR). The FTIR operates by transmitting light through the test sample at the mid-infrared band and recording the energy of light absorbed by the material at specific wavelengths. The absorbed light at a certain wavelength is characteristic of the chemical bonds which make up the material's structure. An absorbance spectrum, which is a plot of percent absorbance versus

wavenumber (reciprocal of wavelength) unique to each compound present was obtained and compared to a library of known spectra for identification.

Mineralogy analysis and determination of TOC content of the shales were performed at the Integrated Core Characterization Center (IC^3) laboratory of the University of Oklahoma.

3.1.3 Native Moisture Content

The native moisture content of a shale sample is defined as the ratio of the mass of water contained in the shale to the total weight of the shale. In other words, it is the fraction of the shale's total mass observed from water contributions. It is usually expressed as a percentage and is calculated using the following equation.

$$NMC\ (wt\%) = \frac{W_w}{W_s} \times 100 \qquad \text{..... (3.2)}$$

where,

$NMC = native\ moisture\ content\ \ (\%)$

$W_w = weight\ of\ \ water\ removed\ by\ drying\ \ (g)$

$W_s = weight\ of\ shale\ sample\ before\ drying\ (g)$

The native moisture content of the shale samples was determined by weighing 4-8 Tyler Equivalent Mesh Size of the shales and drying in an oven at 150˚F to constant weight. The drying process removes attached water molecules which makeup the shale's native moisture content.

3.1.4 Cation Exchange Capacity

The cation exchange capacity (CEC) of shale is very important in its characterization. CEC is a function of the amount and type of clay mineral present in shale. The higher the CEC of a clay mineral, the more reactive it is. Therefore, since shales contain clay minerals, their reactivity can be deduced from their CEC. The CEC of the shales were determined using the methylene blue method. This method involves the titration of clay suspensions using the methylene blue dye. The method was first developed by Jones (1964) for determining the bentonite content of drilling fluids and was later modified by Osisanya and Chenevert (1991) for shales. Methylene blue is an organic dye that readily displaces exchangeable cations present in the clay minerals. As it replaces these cations, it is absorbed into the clay particles.

The shale samples were ground to 100-200 Tyler Equivalent Mesh Size. Ten (10) grams were weighed out and dispersed in 350ml of deionized water using a multimixer for fifteen (15) minutes. Two (2) milliliters of the mixture was transferred into a 250 ml Erlenmeyer flask using a syringe. Ten (10) milliliters of deionized water was added and the resulting mixture treated with 15 ml of 3% hydrogen peroxide (H_2O_2) and 0.5 ml of 5N sulfuric acid (H_2SO_4). Hydrogen peroxide oxidizes any organic matter as they too absorb the methylene blue dye. After boiling gently for ten (10) minutes, the mixture was diluted to 50 ml with deionized water.

The mixture was titrated against reagent grade 0.01M methylene blue solution. The dye was added in increments of 0.5 ml and drops of the solution were placed on filter paper (Whatman Grade 1) until a purple halo was observed around the solids as shown in Figure 3.1. This halo signifies the complete absorption of methylene blue dye on all the

available exchangeable sites possessed by the shale. It is also known as the endpoint of the titration.

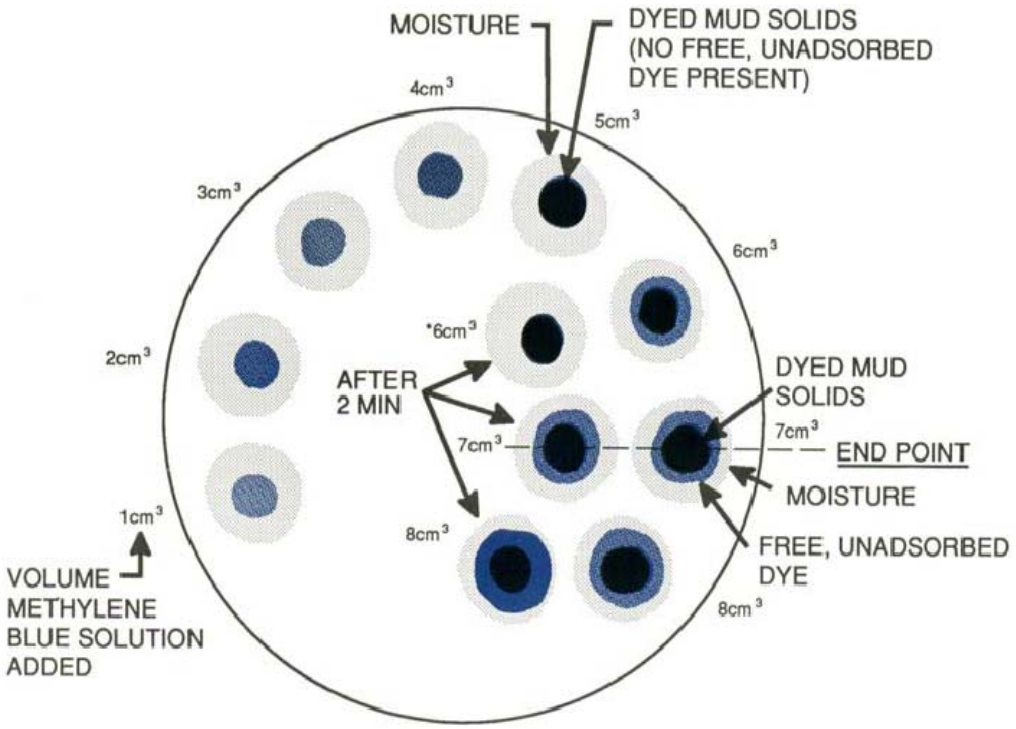

Figure 3.1: Spot Test for Endpoint of Methylene Blue Titration

3.2 Adsorption Isotherm

3.2.1 Concept: Isopiestic Method

Adsorption measurements have been made using a variety of experimental procedures (Gruszkiewicz et al 2005).They include the static volumetric method, the dynamic (gas flow) method and the static gravimetric method.

For simplicity and accuracy, the static gravimetric method, also known as the isopiestic method was used to develop the shale adsorption isotherms. In this method, weight measurements are taken of shale samples under varying relative humidity conditions at constant temperature and pressure. The relative humidity environments were created using saturated salt solutions in desiccators. The moisture adsorbed physically is the difference between the water content as expressed in initial weight and the water content at equilibrium known as the final weight of the sample. For this study, tests were carried out at ambient conditions. High temperature, high pressure tests are beyond the scope of this work.

3.2.2 Preparation of Saturated Salt Solutions

The saturated salt solutions were prepared by dissolving reagent grade salts in 400 ml of deionized water. The salts include zinc chloride ($ZnCl_2$), Calcium Chloride ($CaCl_2$), Calcium Nitrate tetrahydrate ($Ca(NO_3)_2.4H_2O$), Sodium Chloride (NaCl), Potassium Chloride (KCl), and Potassium Phosphate (KH_2PO_4). The amounts of each salt required to produce a saturated solution was determined from their solubility at room temperature printed in the CRC Handbook of Chemistry (2004). To guarantee complete saturation, visible salt particles were observed at the base of the solutions in the desiccators. Despite publications (Resnik et al 1984, Labuza et al 1976, Chenevert 1970) on the relative

humidity environments provided by each saturated salt, in this study measurements at room temperature were carried out to ensure accurate isotherms. A Traceable hygrometer measuring humidity ranges from 10.00 to 95.00 % with an accuracy of ±4 % was used. The probe was suspended above the solutions in a closed system created by 250 ml flask sealed with a cork. A hole was drilled into the cork small enough to tightly fit the probe through. Table 3.1 shows the results of the water activities obtained for the saturated salt solutions compared to literature values.

Table 3.1: Water Activity of Saturated Salt Solutions (After O'Brien and Chenevert 1973)

Saturated Salt Solution	Water Activity (Literature)	Water Activity (Laboratory)
Zinc Chloride ($ZnCl_2$)	0.100	0.11
Calcium Chloride ($CaCl_2$)	0.295	0.30
Calcium Nitrate tetrahydrate ($Ca(NO_3)_2.4H_2O$)	0.505	0.51
Sodium Chloride (NaCl)	0.755	0.76
Potassium Chloride (KCl)	0.860	0.86
Potassium Phosphate (KH_2PO_4)	0.960	0.96

3.2.3 Adsorption Isotherm Tests

The shale samples used in the determination of native moisture content were promptly ground to 100-200 Tyler Equivalent Mesh Sizes and dried in an oven for 24 hours at 150˚F. The saturated salt solutions (Table 3.1) prepared previously were placed in well labeled desiccators. Plastic (Nalgene) and Dry-seal glass (Wheaton) vacuum desiccators equipped with a stopcock for vacuum pulling were used.

The following steps were carried out for the adsorption isotherm experiment:

1. Transfer 400ml of the prepared saturated salt solutions into separate well-labeled vacuum desiccators and position the plate above the solutions.
2. Place convenient weights of the dried shale samples in petri-dishes on the desiccators' plate above the salt solutions as shown in Figure 3.2.
3. Grease the desiccators' edges with silicon-based high vacuum grease to ensure total exclusion of air and cover the desiccator.
4. Pull a vacuum on the desiccators using a vacuum source by connecting it to the desiccators' stop cock. When a proper vacuum has been applied, the solution begins to bubble up. This occurs because at lower pressures produced by the vacuum, the vapor pressure of a liquid will equal the pressure above it and boiling will occur.
5. On a daily basis, quickly remove and weigh shale samples using a mass balance. Place them back in the desiccators, repeating step 4. Record weight changes until they are negligible. At this time, equilibrium has been reached and the shale no longer adsorbs water from that activity atmosphere.

Each shale sample took between five to seven days for equilibrium to be reached.

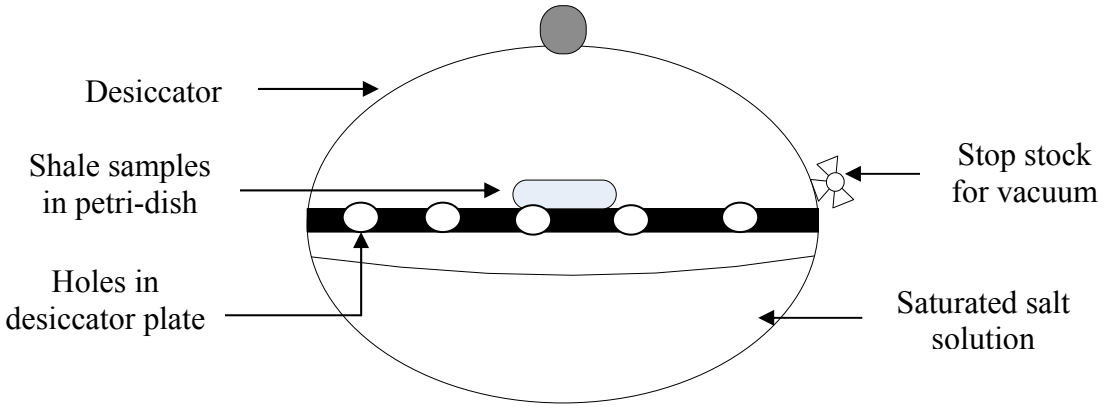

Figure 3.2: Shale Sample in Desiccator

The percent moisture adsorbed by the shale was calculated using the following equation:

$$MC\ (wt\%) = \frac{W_w}{W_s} \times 100 \qquad \text{..... (3.3)}$$

where,

$MC = moisture\ content\ (\%)$

$W_w = weight\ gained\ by\ shale\ sample\ (g)$

$W_s = weight\ of\ dried\ shale\ sample\ (g)$

The adsorption isotherms were developed by plotting the weight of adsorbed moisture versus the aqueous activities of the saturated salt solutions.

Several arguments have been raised on the accuracy of this methodology. Taking the shale out to measure its weight causes a change in the desiccator's environment. This was minimized by weighing the shale as quickly as possible. Special control humidity environments in which mass balances are incorporated have been created to ensure a consistent atmosphere. However, these were not available for this study.

3.3 Development and Evaluation of Water Based Mud

One of the main objective of this study is to develop a water based mud that will minimize shale dispersion and swelling for the shale samples obtained. Several water based fluid systems have been developed and tested for various shale samples as discussed in the literature review. However, each shale formation requires a unique drilling fluid for effective inhibition.

3.3.1 Fluid Design and Test Matrix

The fluid design is based on common oilfield materials. They include three salts, (1) Potassium chloride, (2) Sodium Chloride, (3) Calcium Chloride, and (4) Bentonite, (5) a polymer, Partially hydrolyzed polyacrylamide (PHPA). Special fluids using Xanthan Gum and a relatively new compound introduced for shale inhibition called Methyl Glucoside (MEG) were also tested. The salts were used to reduce the fluids chemical potential while the polymer was used as an encapsulator and a viscosifier.

In total, 7 mud systems were formulated for each bentonitic and polymeric mud. Table 3.2 shows the compositions of the developed test fluids.

Table 3.2: Compositions of Developed Test Fluids

Base Fluid = *Water (350ml)+ 0.25g NaOH* *Density = 8.34 lb/gal* pH = *10-11*			
	Mud System	**Composition**	**Density lb/gal**
	Base Fluids		
1		4% Bentonite	8.55
2		1 ppb PHPA	8.35
	KCl-Bentonite Mud		
3		4% Bentonite + 0.5% KCl	8.55
4		4% Bentonite + 1% KCl	8.60
	KCl-PHPA Mud		
5		1ppb PHPA + 0.5% KCl	8.35
6		1ppb PHPA + 1% KCl	8.40
	NaCl-Bentonite Mud		
7		4% Bentonite + 0.5% NaCl	8.55
8		4% Bentonite + 1% NaCl	8.60
	NaCl-PHPA Mud		
9		1ppb PHPA + 0.5% NaCl	8.35
10		1ppb PHPA + 1% NaCl	8.35
	$CaCl_2$-Bentonite Mud		
11		4% Bentonite + 0.5% $CaCl_2$	8.50
12		4% Bentonite + 1% $CaCl_2$	8.55
	$CaCl_2$-PHPA Mud		
13		1ppb PHPA + 0.5% $CaCl_2$	8.35
14		1ppb PHPA + 1% $CaCl_2$	8.45
	Special Fluids		
15		2ppb PHPA + 1% KCl	8.45
16		2ppb Xanthan Gum + 1% KCl	-
17		2ppb PHPA + 20% *MEG*	8.85

- **Fluid was foamy and bubbles could not be removed**

3.3.2 Dispersion Tests

Shale dispersion is a process by which shale cuttings disintegrate into smaller sizes usually described as fines. It is a function of mechanical factors such as shear and chemical factors such as hydration. A shale's dispersive abilities vary depending on the fluid in contact with it. A fluid will successfully inhibit dispersion by preventing the shale from breaking into smaller pieces. In this study, dispersion tests were performed to investigate the inhibitive properties of the prepared drilling fluids with the shale samples. The drilling fluid's ability to maintain the cuttings integrity and the temperature effects on drilling fluid properties such as viscosity were analyzed.

Apparatus/Equipment/Materials

Dispersion tests were carried out using a five roller hot-rolling oven and 500 ml high temperature aging cells made from stainless steel. The oven contained a horizontal rack of cylinders which rolled at 25 RPM. The oven was also equipped with a digital temperature controller (100-450˚F) and a timer. The shale samples used were ground to 4-8 Tyler Equivalent Mesh sizes as this size is representative of cuttings observed on the drilling field.

Procedure

Ten (10) grams of 4-8 Tyler Equivalent Mesh size shale were weighed and placed into the aging cells. Care was taken not to expose the samples to air for too long in order to prevent dehydration. 350 ml of the prepared drilling fluid was added to the shale cuttings in the aging cell and the container properly closed. Loading of the aging cells did not exceed 75% of their total volume as this gave room for possible thermal expansions. The contents of the aging cells were hot rolled for 16 hours after which the residual

cuttings were washed and screened through a 0.023 inch (0.584mm) mesh size. Smaller sizes were considered irrecoverable and described as fines dispersed in the drilling fluid. The recovered cuttings were dried to constant weight for 24 hours. Tests were run at ambient temperature (75˚F) and elevated temperatures of 150˚F and 200˚F for all the drilling fluids. Fluids 1-14 from Table 3.2 were used in the dispersion test. A schematic of the rolling process is shown in Figure 3.3.

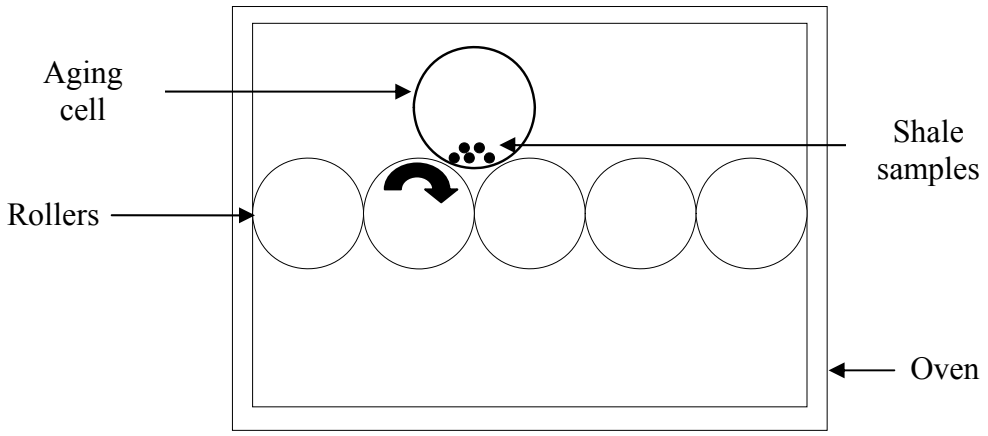

Figure 3.3: Shale in Hot Roller Oven

Percent Recovery observed from the tests was calculated using the following equation:

$$P\ (\%) = \frac{W_u}{W_s} \times 100 \qquad \text{……...……... (3.4)}$$

where,

$P = percent\ recovery\ (\%)$

$W_u = weight\ of\ undispersed\ shale\ (g)$

$W_s = original\ weight\ of\ shale\ sample\ (g)$

Fluid rheological properties were also measured using a six speed Fann 35 viscometer before and after dispersion tests. This was done in order to monitor rheological alterations due to shale disintegration and temperature changes after dispersion test were carried out. Other fluid properties such as the density and pH were measured using a mud balance and pH paper.

3.3.3 Swelling Tests

Based on dispersion tests and rheological properties, fluids 15-17 from Table 3.2 were used for swelling tests carried out at ambient conditions (75˚F). Shales swell when in contact with aqueous fluids due to their clay content. The swelling is physically observed as an expansion from their original size. Swelling can be measured in a number of different directions, however, linear expansion is most representative of the increase seen by the wellbore. It is measured in the direction perpendicular to the bedding plane as this is the direction of swelling into the wellbore. Swelling tests directly measure the effect of shale-fluid interaction in the form of linear swelling.

Apparatus/Equipment/Materials

For this study, a simple but unique device created at the University of Oklahoma's Drilling Laboratory was used to measure shale swelling. It was chosen due to its portability, direct-reading capability from the gauge screen and eliminated need for calibration. Figure 3.4 shows the equipment used. It consists of two major parts: (1) an immersion chamber and (2) a digital micrometer. The immersion chamber was made from plexi-glass equipped with a flexible pin that extends beyond the chamber. Within the chamber, the shale is held in place between the pin and the chamber wall. The digital micrometer was held against the other end of the pin using a clamp. The micrometer

measures with a 0.0005 inches resolution upon pressure application. Figure 3.5 shows a schematic of the swelling process and measurement. A saw was used to cut the shale into slabs and a sander used to polish both sides of the shale surface. An even surface is essential in order to capture a uniform linear swell.

Procedure

The dimensions of the slabs were measured using vernier calipers to the nearest 0.001inches. An initial length of 0.25 inches was used for the shale slabs. The shale was then placed in the immersion chamber and held in place by the pin. The test fluid was poured into the chamber to completely immerse the shale but leave the pin free to respond to shale swelling. Immediately, a timer was started and changes in the reading shown on the micrometer were recorded at convenient time intervals. De-ionized water was used as the base fluid for this experiment before the test fluids were evaluated.

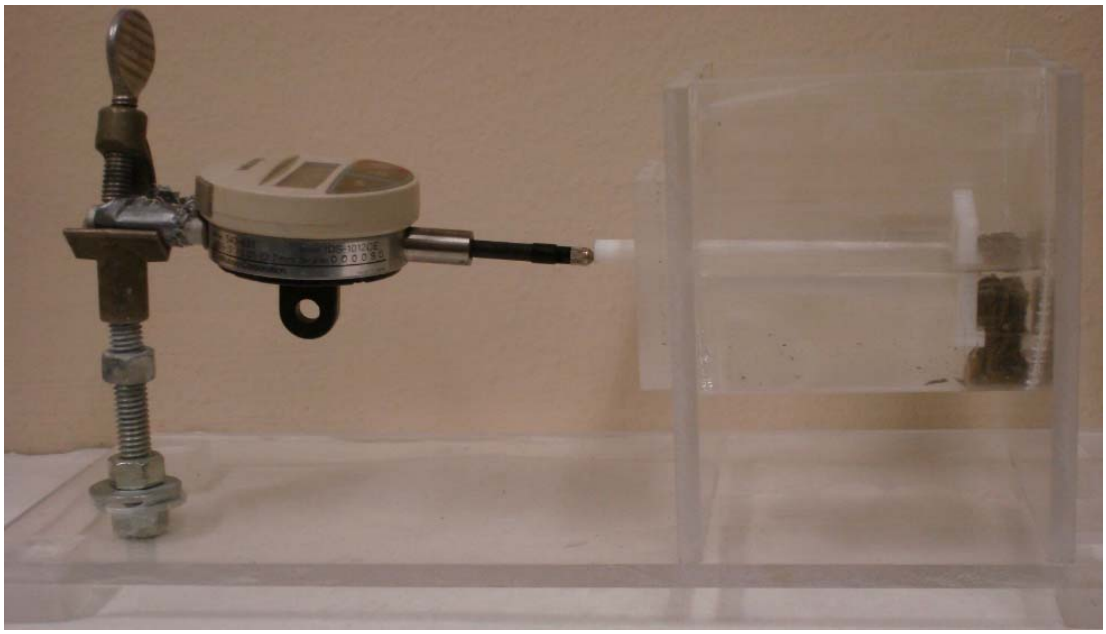

Figure 3.4: Digimatic Indicator and Immersion Chamber

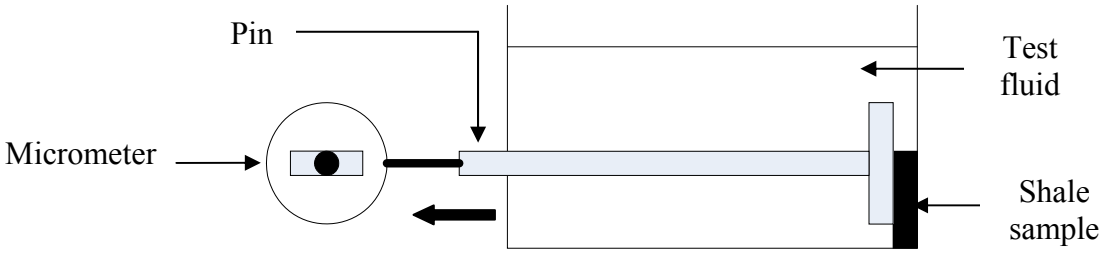

Figure 3.5: Schematic of Swelling Apparatus

Measurements were taken over a period of 24 hours and converted to percent linear swell using the following equation:

$$\varepsilon\ (\%) = \frac{\Delta L}{L} \times 100 \qquad \text{..... (3.5)}$$

where,

$\varepsilon = percent\ linear\ swell\ (\%)$

$\Delta L = change\ in\ \ shale\ length\ \ (in)$

$L = original\ length\ of\ \ shale\ sample\ \ (in)$

CHAPTER 4: EXPERIMENTAL RESULTS AND DATA ANALYSES

This chapter presents the data analysis, results and discussions from the experiments described in Chapter 3. It also provides detailed analysis of the outcomes observed. All raw data from the various experiments are recorded in Appendix A.

4.1 Shale Characterization

4.1.1 Mineralogy

Mineralogy analysis indicates the relative quantities of compounds present in a rock. Clay and non-clay minerals are usually present in shales. The type of clay present is an indication of the degree of hydration experienced by the shale. Furthermore, it can be used to estimate the severity of wellbore instability issues that may arise. The mineralogy analysis for both the Barnett and Norway shales are presented in Table 4.1. The Barnett shale cored at a depth of 6627.5 ft - 6629.3 ft, is made up of 49% clay and 32% Quartz. It contains other non-clay minerals such as feldspar and carbonates in minimal amounts. The bulk of the clay content consists of 26% illite, mixed clays of 22% and 1% chlorite. Zero smectite levels indicate low swelling tendencies. According to the classification by O'Brien and Chenevert (1973) based on clay content distribution, the Barnett shale falls in the fifth class. The shales in this classification have high illite and moderate chlorite content. They are hard and brittle in nature with no significant dispersion. However, caving tendencies are highly probable.

The Norway shale is composed of 57% clays and 26% feldspar. Negligible amounts of other non-clay minerals are present. Among the clays are 41% illite, kaolinite (9%) and smectite (6%), 1% mixed clays. The existence of smectite indicates the

probability of some swelling and dispersion in aqueous solution. The Norway shale falls in the second class of shales according to O'Brien and Chenevert (1973). The second class shales have moderate smectite and high illite content. They are soft and exhibit fairly high dispersion.

Table 4.1: Shale Sample Mineralogy

Depth Interval (ft):	**Barnett** 6627.5 - 6629.3	**Norway** 7072 - 7075
Quartz	32	8
Carbonates	5	4
Feldspar	9	26
Pyrite	1	0
Anhydrite	0	1
Apatite	4	4
Clays	49	57
Illite	26	41
Smectite	0	6
Kaolinite	0	9
Chlorite	1	0
Mixed Clays	22	1

4.1.2 Native Moisture Content (NMC), Cation Exchange Capacity (CEC) and Total Organic Carbon Content (TOC)

Table 4.2 shows the test results for NMC, CEC, and TOC for the Barnett and Norway shales. The native moisture content obtained for the Barnett shale was 0.3 % while a value of 18.9% was recorded for the Norway shale. The Norway shale contains more moisture than the Barnett shale and is expected to have a higher isotherm curve and native activity. Moisture content is a function of various factors with the most important being clay mineral composition and preservation techniques. High moisture contents

indicate the presence of expandable clays with the ability to store moisture by adsorption. Furthermore, unpreserved shales loose their in-situ moisture when brought to the surface because of the change in environmental conditions. Acceptable preservation techniques include immersion in oil or coating with wax. The Barnett shale was collected in polythene bags and contains no smectite therefore it yielded a lesser value of native moisture content.

CEC was calculated from the results of the methylene blue tests using the following equation:

$$CEC = \frac{C_D \times V_{MB} \times C_{MB}}{V_{DF} \times M_S} \quad \text{……...…….. (4.1)}$$

where,

$CEC = cation\ exchange\ capacity\ (Meq/100g\ of\ solid)$

$V_{MB} = volume\ of\ methylene\ blue\ titrated\ (ml)$

$C_{MB} = concentration\ of\ methylene\ blue\ solution\ (M)$

$V_{DF} = volume\ of\ dispersed\ fluid\ (ml)$

$M_S = mass\ of\ shale\ dispersed\ (g)$

$C_D = volume\ cons\tan t$

Table 4.2: Native Moisture Content, Cation Exchange Capacity, and Total Organic Content Values

	Barnett	**Norway**
Native Moisture Content (% weight)	0.3	18.9
Cation Exchange Capacity (Meq/100gm of Solid)	4.4	9.6
Total Organic Content (%)	2.9	6.1

CEC values for the Barnett and Norway shales are 4.4 and 9.6 meq/100gm of solid respectively. The presence of smectite in the Norway shale creates an increased surface area for adsorption of the methylene blue dye, thus the higher CEC value. Other common clay minerals such as illite and chlorite have lower CEC's due to their rigid structures. Therefore, they do not adsorb much of the dye. The total organic carbon content values for Barnett and Norway shales are 2.9% and 6.1% respectively. Organic matter, similar to smectite has a high surface area and can store moisture significantly. This also accounts for the high native moisture content value observed for the Norway shale.

4.2 Adsorption Isotherms

Adsorption isotherms (Figures 4.1 and 4.2) provide information on a material's water content at certain equilibrium conditions. The behavior of a shale sample under these conditions can directly be related to its hydration and swelling potential. The isotherm can also give information on the expandable clay content of the shale. Two vital pieces of information are needed from the adsorption isotherm in order to make these conclusions. First, the shape of the adsorption isotherm, for compositionally and structurally similar clays, should approximately be similar to one of the already established isotherms (Chapter 2). This validates the result. Second, the amount of moisture adsorbed that is expressed on the y-axis of the curve shows which shale is more likely to hydrate. This can be confirmed from mineralogy test analysis.

4.2.1 Results

The adsorption isotherm for the Barnett Shale sample is shown in Figure 4.1. The shape is similar to the Type II sigmoidal BET isotherm. Several authors including Chenevert (1970), Osisanya (1991), and Oleas et al. (2008) have reported isotherms with similar Type II shape. Using the native moisture content obtained previously as 0.3% and the adsorption isotherm, we can obtain the equilibrium activity of approximately 0.4.

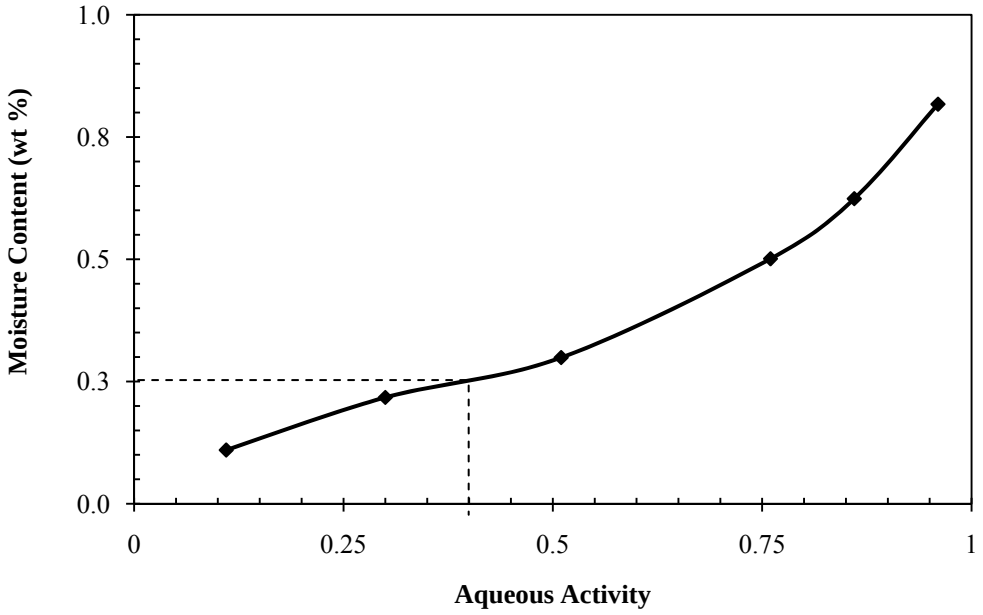

Figure 4.1: Adsorption Isotherm for Barnett Shale

Figure 4.2 shows the adsorption isotherm for the Norway sample. The shape observed is characteristic of the Type III BET isotherm. Isotherms of this nature are commonly found in foods with soluble components e.g. sugars (Rizvi 1986, Hui et al. 2006). This shape is an evidence of organic matter present in the shale because organic matter is soluble in water. An equilibrium activity of approximately 0.92 was obtained from the native moisture content and the adsorption isotherm.

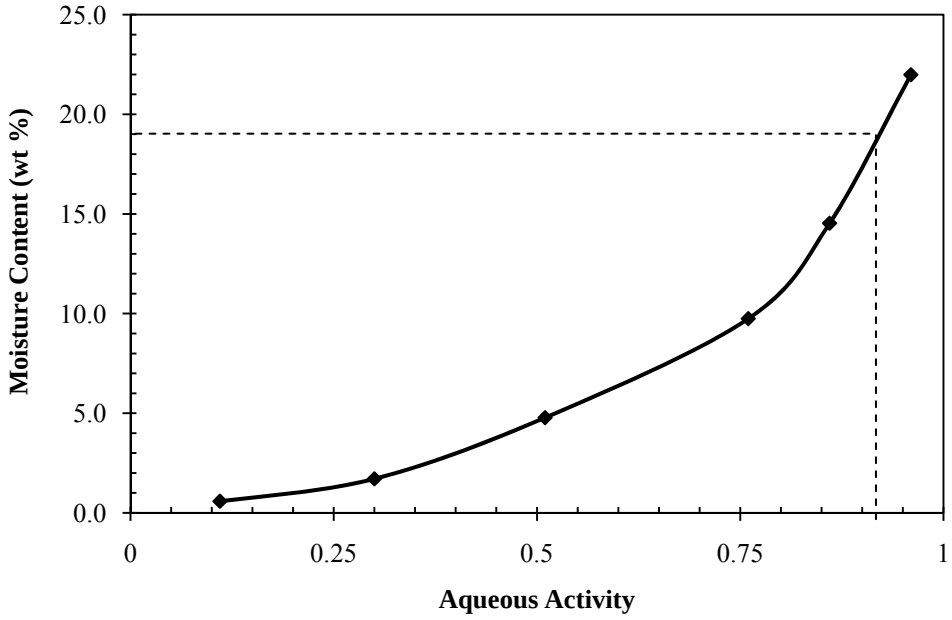

Figure 4.2: Adsorption Isotherm for Norway Shale

Figure 4.3 shows a comparison of the Barnett and Norway isotherms. It indicates that Norway shale has a higher adsorptive potential than the Barnett shale. A conclusion that more adsorption took place in this shale than in the Barnett shales can be made, therefore more expandable clays are present. This is confirmed by the mineralogy results which showed the presence of highly expandable clay (smectite) within the Norway shales.

4.2.2 Modeling of Adsorption Isotherms

Adsorption isotherms, though they illustrate the reactive potential of shales, have not been modeled to predict the reactivity of clays. In the food industry, several models have been developed to describe isotherms of food products. The Guggenheim, Anderson and DeBoer (GAB) model being the most commonly accepted model was used to fit the isotherms of the Norway and Barnett shales. This model has two advantages over the BET model. It fits a wider range of activity values between 0-0.99 (Singh and Singh 1996) compared with the BET which only fits activities below 0.45 (Wang and Padua 2004). Moreover, the flexibility of the GAB isotherm has been attested through various literatures (McMinn and Magee 1999). That is, it fits a wide variety of materials. Other shale adsorption isotherms developed by Osisanya (1991) for Mancos, Wellington and Pierre shales were also fitted. This was done to investigate any possible trend with shale type and GAB model parameters. More shale types explored creates a stronger validation of any observed trends.

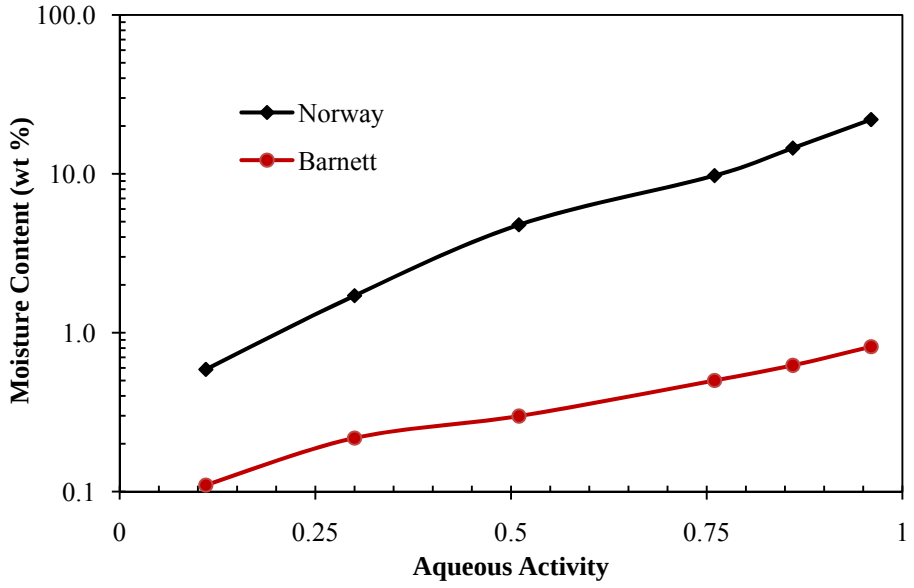

Figure 4.3: Comparison of Barnett and Norway Shale Adsorption Isotherms

The GAB model equation is expressed as follows:

$$W = \frac{CKW_m}{(1-Ka_w)(1-Ka_w+CKa_w)} \quad \text{……...…….. (4.2)}$$

Input Values

W = moisture content of the material on a dry basis (kg/kg % dry matter)

a_w = water activity

Parameters And Constants

W_m = moisture content corresponding to saturation of all primary sites by one molecule of water (monolayer moisture on a dry basis) (kg/kg % dry matter)

C = guggenheim constant
= $C_o \exp(\Delta h_c/RT)$

K = factor for multiple layers of molecules with respect to bulk liquid
= $K_o \exp(\Delta h_k/RT)$

Δh_c = specific bonding enthalpy of water monolayer (J/kg)
= $\Delta h_{s,\,mono} - \Delta h_{vap}$

Δh_k = mean specific bonding enthalpy of the water multilayer (J/Kg)
= $\Delta h_{s,\,multi} - \Delta h_{vap}$

R = universal gas constant (J/kg/K)

T = absolute temperature (K)

$\Delta h_{s,\,mono}$ = specific sorption enthalpy of water monolayer (J/kg)

Δh_{vap} = specific vaporization enthalpy of water(J/kg)

$\Delta h_{s,\,multi}$ = mean specific sorption enthalpy of the water multilayer (J/kg)

C_o and K_o = adjustable parameters accounting for temperature effect

The most important parameter in the model is the monolayer moisture content W_m. Reactive clay minerals such as smectite have a higher number of active interlayers and increased isomorphic substitution than less reactive clays. Shales with higher reactive clays will therefore have more area for monolayer coverage by water molecules before multiple layers begin to form. Thus the W_m will be higher for reactive shale like the Norway shale and lower for less reactive shale like the Barnett.

A windows software called LABfit was used to fit the curves to the model equation. The program uses a nonlinear regression-least squares method for curve fitting. Experimental data was inputted into the program along with the model equation and analysis carried out. The square of the correlation coefficient (R^2) for the fit ranged between 0.98 and 1.00 showing a good fit by the model. Figures 4.4 – 4.8 show the adsorption isotherms obtained from experimental data and the GAB model. Table 4.3 gives the W_m of each shale from the model along with the value of the CEC previously obtained.

Table 4.3: Cation Exchange Capacities and Monolayer Moisture Content for Various Shales

	Barnett	**Mancos**	**Wellington**	**Norway**	**Pierre**
CEC (Meq/100g of Solid)	4.37	6.5	9.28	9.6	17.5
W_m (kg/kg % Dry Basis)	0.1701	0.3554	1.031	4.568	1.547

The CEC and W_m values appear to exhibit a trend for all the shales except the Norway shale. Higher CEC values were observed with higher monolayer moisture values. A correlation might exist between these CEC and W_m values, however, the first step to a conclusion is to clarify the discrepancy observed by the Norway shale. Fenema

(1996) and Fellows (2000) acknowledged the dependence of adsorption isotherm properties on composition, physical structure, method of pretreatment, temperature and preparation methodology of the samples tested. The only differences between the shales used were their composition and preparation methodology. Along the composition perspective, Udy (1976) observed an increase in adsorption based on elevated amounts of organic content in soils. The total organic content (TOC) for the Norway shale and the Barnett shale were 6.1% and 2.9% respectively. These values fully support the theory that the organic content plays a part in the adsorption isotherm shape and higher monolayer moisture content observed for the Norway Shale.

Several experiments with soil protein adsorption by Russell (1982) also concluded that a complex adsorber like soil could vary in adsorbance due to organic content, cation exchange capacity, and nature of exchangeable cations. Therefore a direct correlation between CEC and monolayer moisture will be skewed when one or more of these properties vary. Most literature reported shale swelling and dispersion tendencies as solely due to CEC, isomorphous substitution and basal spacing. This tendency may also be due to organic matter present in the shale. Graber et al. (2003) also confirmed this by highlighting the effect of water sorption onto organic matter. The presence of water solvates organic matter. This creates multiple adsorption sites resulting in increased adsorption isotherm values.

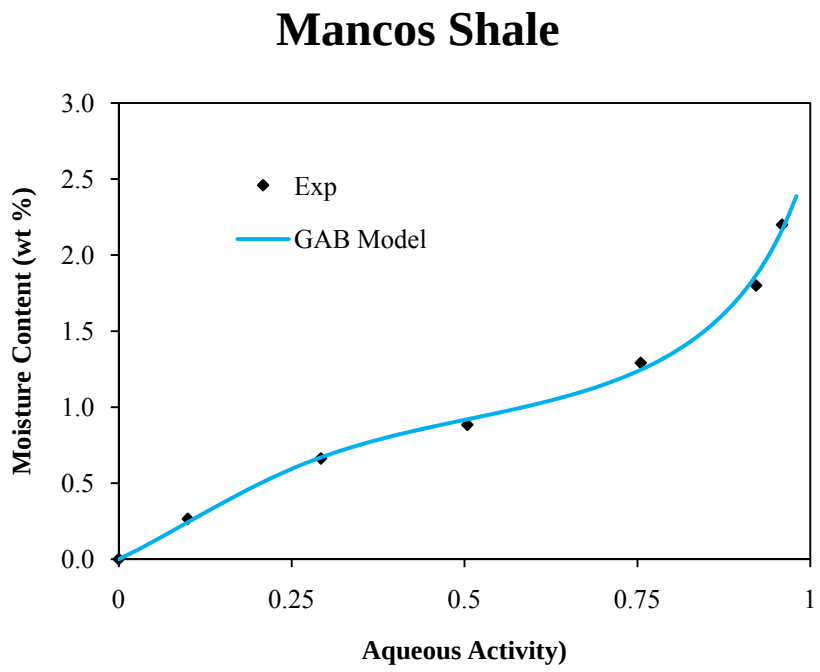

Figure 4.4: Adsorption Isotherm of Mancos Shale fitted to the GAB model

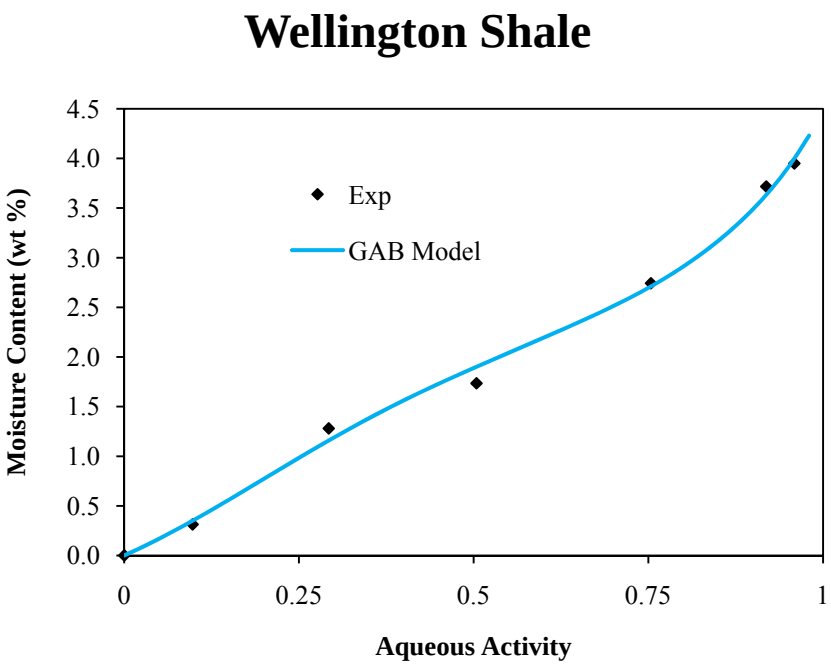

Figure 4.5: Adsorption Isotherm of Wellington Shale fitted to the GAB model

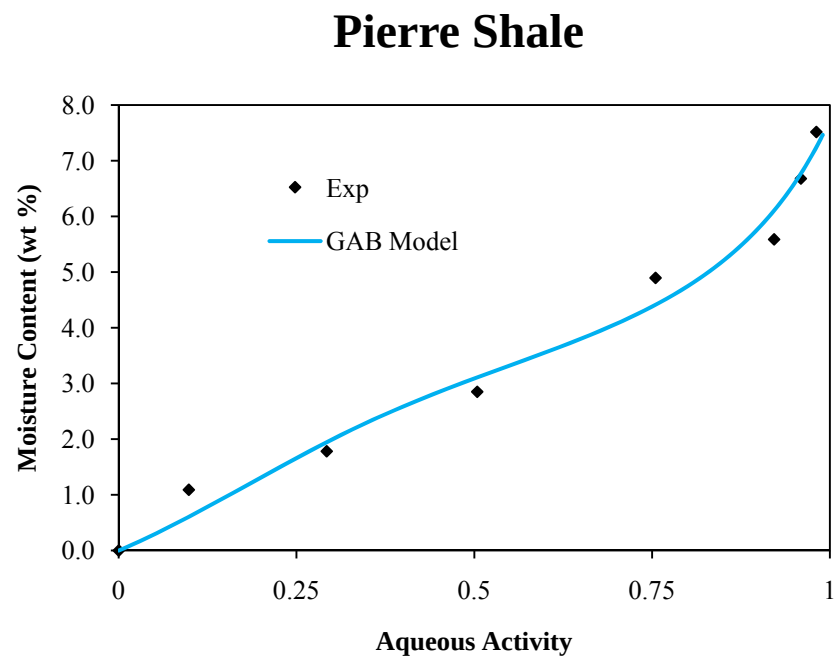

Figure 4.6: Adsorption Isotherm of Pierre Shale fitted to the GAB model

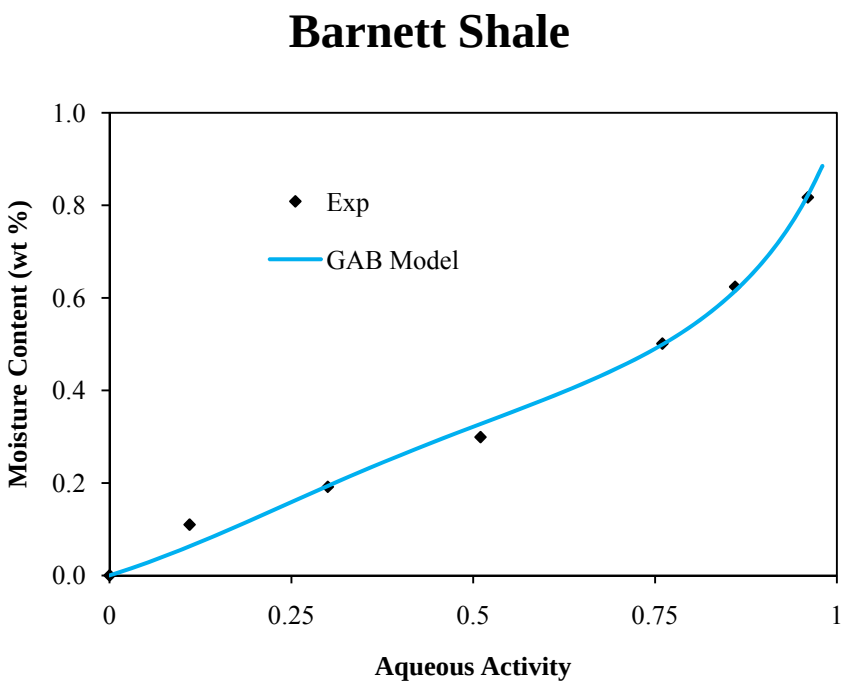

Figure 4.7: Adsorption Isotherm of Barnett Shale fitted to the GAB model

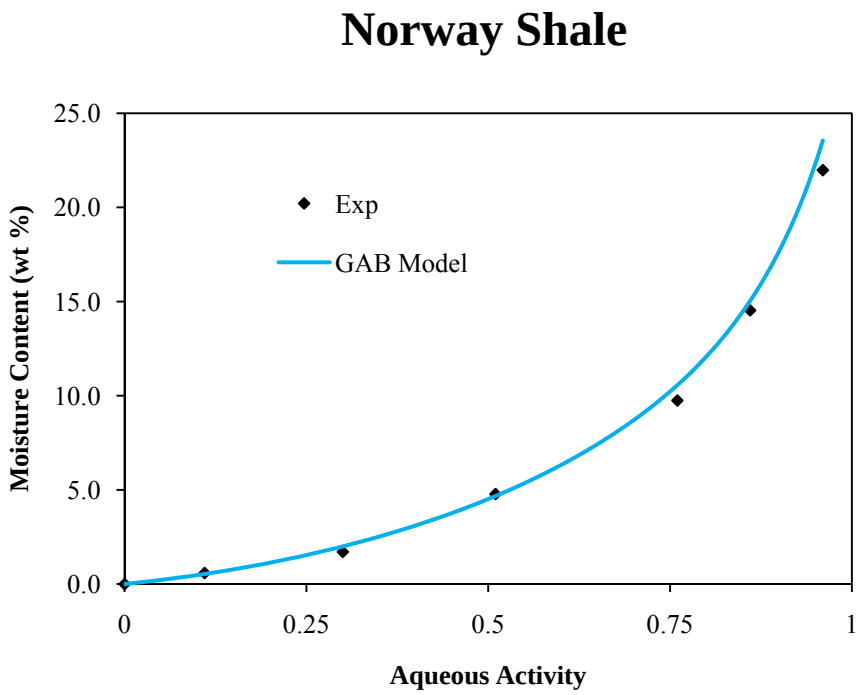

Figure 4.8: Adsorption Isotherm of Norway Shale fitted to the GAB model

Another application of adsorption isotherm modeling is the determination of properties at temperatures other than the ambient. Most shale isotherms have been developed under ambient conditions. This is however not representative of in-situ conditions. Generally, increased temperature will reduce adsorption to some degree (Hui et al. 2006). Thus, activity values claimed to correctly balance the aqueous phase of the drilling fluid may in fact be incorrect. These isotherms can be obtained by placing samples in a constant environment chamber at various temperatures and relative humidities. They can be curve-fitted to the GAB equation using the approach presented. The temperature dependent parameters, C and K, can then be evaluated based on their variations with temperature. Once a trend is established, predictions can be made for downhole temperatures. Adsorption isotherm variations with temperature, if significant,

will imply that activity values obtained from ambient conditions are not representative of in-situ activity. Thus, disproving the activity concept as the major driving force in balanced activity OBMs. This information can be applied to improve the development of WBM of similar qualities as OBMs.

4.3 Shale-Drilling Fluid Interaction

4.3.1 Dispersion Test Results

Dispersion tests were carried out using various fluids for the Norway shale at different temperatures. The Norway shale experienced more dispersion (Table 4.4) as predicted by the classification offered by O'Brien and Chenevert (1973). The Barnett shale exhibited no dispersion after testing with deionized water. This is expected as the shale is hard. As a result, dispersion tests for the Barnett shale were terminated. However, other problems such as caving due to rock stresses, cannot be measured in the laboratory may be observed while drilling through the Barnett shale.

Percent recovery, a measure of shale recovered after dispersion tests, was calculated. Table 4.4 shows the percent recoveries for the bentonitic fluids. It shows that all fluids exhibited higher recovery compared to the base fluid composition. Clearly, maximum recovery was obtained using a fluid composition of *Base fluid + 1% KCl*. At all temperatures, this fluid produced the highest recovery. For all the bentonitic fluids, percent recoveries were higher at 75˚F than those obtained at 150˚F. At higher temperatures, the weakening of bonds between molecules due to increased molecular vibrations results in increased water movement into the shale structure. Thus more shale disintegrates into fines and the percent recovery is reduced. However, the percent

recovery values at 200˚F are higher than those obtained 150˚F. The subsequent increase at 200˚F could be as a result of changes in fluid rheology at that temperature.

Table 4.4: Norway Shale Percent Recoveries for Bentonitic Fluids

Base Fluid: Tap water + 4% Bentonite				
Mud System	**Composition**	**% Recovery**		
		Ambient (75 ˚F)	**150 ˚F**	**200 ˚F**
Bentonite Slurry	Base Fluid	60.3	43.0	44.9
KCl/Bentonite	0.5% KCl	71.6	70.8	77.1
	1% KCl	77.9	77.3	77.8
NaCl/Bentonite	0.5% NaCl	65.8	62.9	71.3
	1% NaCl	73.4	73.1	75.9
$CaCl_2$/Bentonite	0.5% $CaCl_2$	70.6	70.4	72.4
	1% $CaCl_2$	77.2	77.0	77.7

Table 4.5 shows the percent recovery values obtained for the polymeric fluids. All fluids performed better than the base fluid. A maximum recovery was obtained with *Base fluid +1% $CaCl_2$*. This fluid gave highest percent recovery at all temperatures: 84.9% at ambient (75˚F), 81.2% at 150˚F and 80.0% at 200˚F. Unlike the bentonitic fluids, as temperature increases, percent recovery reduces for all the temperature ranges used. The ability of polymeric fluids to successfully inhibit shale dispersion is highly temperature dependent. Using the same concentrations as other salts, calcium chloride ($CaCl_2$) gave the highest recovery, thus providing the highest inhibition. This may be due to its low activity environment plus the influence of polymer encapsulation. Polymers hydrate on exposure to water. This hydration causes an increase in their surface area which enables them to effectively coat the shale surface and delay dispersion. This phenomenon is known as polymer encapsulation. This was not the case with the bentonitic fluids because polymers were not added.

It is apparent that at higher temperatures, the percent recoveries obtained from the salt/bentonite fluids show minimal differences. The effect of temperature on percent recovery values may therefore be negligible in these cases. The little variations observed may be an effect of experimental error.

Table 4.5: Norway Shale Percent Recoveries for Polymeric Fluids

Base Fluid: Tap water + 1 ppb PHPA				
Mud System	**Composition**	**% Recovery**		
		Ambient 75 ˚F	**150 ˚F**	**200 ˚F**
Polymer	Base Fluid	61.7	55.6	61.0
KCl/Polymer	0.5% KCl	76.8	76.1	75.1
	1% KCl	77.5	76.8	76.5
NaCl/Polymer	0.5% NaCl	76.2	74.2	71.5
	1% NaCl	77.3	75.5	74.8
$CaCl_2$/Polymer	0.5% $CaCl_2$	82.6	80.4	78.6
	1% $CaCl_2$	84.9	81.2	80.0

Further analysis of the dispersion tests involved the measurement of the fluid rheology before and after the tests. Values of shear stress (τ) and shear rate (γ) were calculated using the following equations:

For shear stress,

$$\tau = 0.01066 \times \theta_i \times N \qquad \text{……...…….. (4.3)}$$

where,

$\tau = shear\ stress\ (lb_f / ft^2)$

$\theta_i = dial\ reading\ at\ i^{th}\ rpm$

$N = spring\ \ factor = 1$

For shear rate,

$$\gamma = 1.703 \times RPM \quad \text{..... (4.4)}$$

where,

$\gamma = shear\ rate\ (1/s)$

$RPM = viscometer\ rotational\ speed$

A rheogram which is a plot of shear stress versus shear rate was developed for the fluids before and after dispersion tests. Figure 4.9 shows the plots for the bentonitic fluids before dispersion tests at 75˚F. Other rheograms are documented in Appendix B. The Base fluid exhibits the Bingham Plastic fluid model while other fluids are yield pseudoplastic in nature, that is they exhibit Power Law fluid model. However, for this study, rheological parameters were determined assuming Bingham Plastic fluid model.

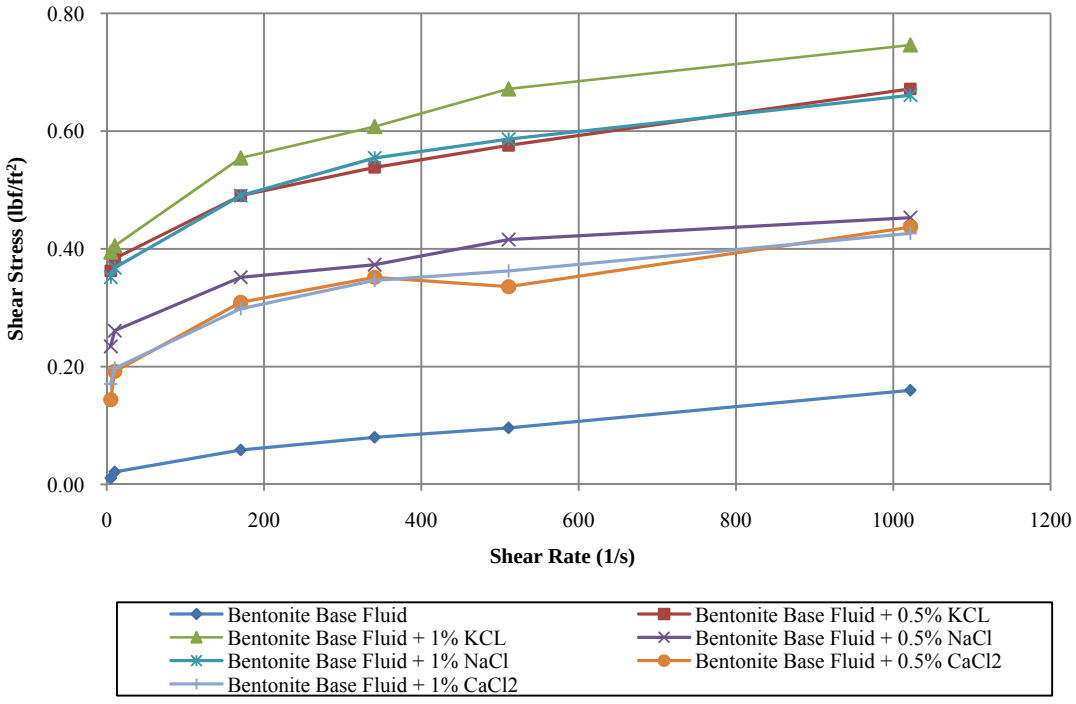

Figure 4.9: Rheogram for Bentonitic Fluids before Dispersion Tests at 75˚F

The plastic viscosity (PV) and yield point (YP) were calculated before and after dispersion using the following equations for a model 35 Fann viscometer with R1B1 and No. 1 spring:

$$\mu_p = \theta_{600} - \theta_{300} \quad \text{..... (4.5)}$$

$$\tau_o = \theta_{300} - \mu_p \quad \text{..... (4.6)}$$

where,

$\mu_p = plastic\ vis\cos ity\ (cp)$

$\tau_o = yield\ stress\ (lb_f/100ft^2)$

$\theta_{600} = dial\ reading\ at\ 600\ rpm$

$\theta_{300} = dial\ reading\ at\ 300\ rpm$

Tables 4.6 and 4.7 show the PV and YP values obtained for the bentonitic fluids. A comparison of the PV values before and after hot-rolling the shale samples showed distinct outcome with the base fluid and the salt/bentonite fluids. The base fluid showed an increase in PV when hot-rolled at all temperatures; which indicates higher shale dispersion (less percent recovery). The salt/bentonite fluids however, exhibited no consistent trend. Generally their PV increased slightly when rolled at ambient conditions then decreased a little at 150˚F. A decrease in PV values was also observed after dispersion tests at 200˚F.

Yield point for the base fluid increased with increasing temperature while the salt/bentonite combinations showed a decrease in YP after hot-rolling at all temperatures. YP is a function of electrostatic forces between fluid particles in motion (Rosco Moss, 1990). For Bingham fluids, it is also the shear stress required to initiate flow in fluids.

From YP results, the dispersion tests reduced the attractive forces between the solid particles significantly.

Table 4.6: Plastic Viscosity Values for Bentonitic Fluids

	Plastic Viscosity (cp)					
	75˚ F		150˚ F		200˚ F	
Fluid Composition	**Before**	**After**	**Before**	**After**	**Before**	**After**
Bentonite Base Fluid	6	9.5	6	8	4	6.5
Bentonite Base Fluid + 0.5% KCl	9	9.5	6.5	7.5	6	2.5
Bentonite Base Fluid + 1% KCl	7	9	3	4	7	7
Bentonite Base Fluid + 0.5% NaCl	3.5	8	6.5	1.5	8	7
Bentonite Base Fluid + 1% NaCl	7	8	7.5	6	7	5.5
Bentonite Base Fluid + 0.5% $CaCl_2$	9.5	3.5	3	2.5	4.5	2
Bentonite Base Fluid + 1% $CaCl_2$	6	4	6	3	5	1

Table 4.7: Yield Point Values for Bentonitic Fluids

	Yield Point ($lb/100ft^2$)					
	75˚ F		150˚ F		200˚ F	
Fluid Composition	**Before**	**After**	**Before**	**After**	**Before**	**After**
Bentonite Base Fluid	3	9	4.5	2.5	4	5
Bentonite Base Fluid + 0.5% KCl	45	5.5	52	7.5	33	9.5
Bentonite Base Fluid + 1% KCl	56	5	92.5	11	39	7
Bentonite Base Fluid + 0.5% NaCl	35.5	9	39.5	9.5	33	7
Bentonite Base Fluid + 1% NaCl	48	6	56	8	40	7
Bentonite Base Fluid + 0.5% $CaCl_2$	22	8.5	15.5	5	30.5	7
Bentonite Base Fluid + 1% $CaCl_2$	28	8	32	9	40	17

Figure 4.10 shows the rheogram for the polymeric fluids before dispersion tests at 75 ˚F. These fluids exhibit a yield pseudoplastic behavior, however, they were also evaluated using the Bingham Plastic model. All other rheograms are shown in Appendix B.

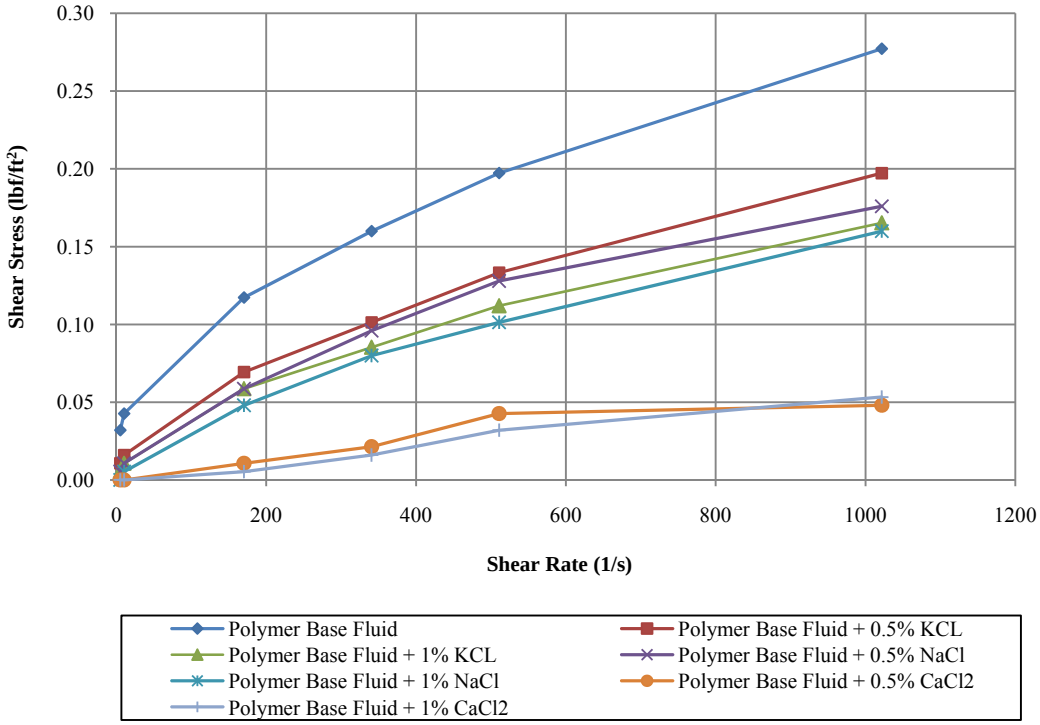

Figure 4.10 : Rheogram for Polymeric Fluids before Dispersion Tests at 75˚F

Table 4.8 and 4.9 show the Plastic viscosity (PV) and yield point (YP) values for the polymeric fluids before and after dispersion tests. Fluids predominantly exhibited a reduction in PV and YP values after dispersion tests. This reduction was more pronounced at higher temperatures. Unlike the bentonitic fluids, polymeric fluids did not show significant changes in these values when dispersion tests were carried out at ambient temperature. Polymeric fluids showed a higher dependence on temperature than the bentonitic fluids.

Table 4.8: Plastic Viscosity Values for Polymeric Fluids

	Plastic Viscosity (cp)					
	75˚ F		150˚ F		200˚ F	
Fluid Composition	Before	After	Before	After	Before	After
Polymer Base Fluid	7.5	7	7	5	6	2.5
Polymer Base Fluid + 0.5% KCl	6	6	6	4	6	2
Polymer Base Fluid + 1% KCl	5	5.5	4.5	4	5	1.5
Polymer Base Fluid + 0.5% NaCl	4.5	5	5.5	5	5	2
Polymer Base Fluid + 1% NaCl	5.5	6	4	4	5.5	1.5
Polymer Base Fluid + 0.5% $CaCl_2$	0.5	0.5	2.5	1.5	3	0.5
Polymer Base Fluid + 1% $CaCl_2$	2	2.5	2.5	0.5	2	1

Table 4.9: Yield Point Values for Polymeric Fluids

	Yield Point ($lb/100ft^2$)					
	75˚ F		150˚ F		200˚ F	
Fluid Composition	Before	After	Before	After	Before	After
Polymer Base Fluid	11	12	17	11	11	0.5
Polymer Base Fluid + 0.5% KCl	6.5	6	7.5	4	6	1
Polymer Base Fluid + 1% KCl	5.5	4.5	4	3.5	5.5	0.5
Polymer Base Fluid + 0.5% NaCl	7.5	6.5	7	2.5	6.5	0.5
Polymer Base Fluid + 1% NaCl	4	4.5	4.5	3.5	4	0.5
Polymer Base Fluid + 0.5% $CaCl_2$	3.5	3	0.5	0	0	0
Polymer Base Fluid + 1% $CaCl_2$	1	0.5	0	0	0	0

4.3.2 Fluid Improvement and Special Fluids Formulation

From the experiments performed, it can be concluded that polymeric fluids excelled in shale inhibition as shown in percent recovery values. Based on the percent recovery and rheological properties the best fluids for the successful inhibition of the Norway shale are *1ppb PHPA + 1% KCl* and *4% Bentonite + 1% KCl*. Further analysis of the *1ppb PHPA + 1% KCl* was carried out by applying several modifications to improve rheological properties. First, the quantity of polymer used was increased from 1ppb to 2 ppb. This improved the YP values immensely. It also increased membrane efficiency for an improved chemical potential mechanism.

Furthermore, Xanthan gum, a water soluble natural polymer was tested as a substitute for synthetic PHPA. Natural polymers are more environmentally friendly than synthetic polymers due to their biodegradability. Also, the Methyl Glucoside (MEG) system acclaimed by Simpson et al (1995) was investigated. The MEG was used in place of KCl due to increasing restrictions over the level of potassium in the drilling fluids especially offshore. Fluids with *2ppb PHPA + 1% KCl*, *2ppb Xanthan Gum + 1% KCl* and *20%MEG + 2ppb PHPA* were tested at 150˚F.

Table 4.10 shows the PV and YP values of the improved and special fluids. All PV and YP values decreased with increasing temperature for *2ppb PHPA + 1% KCl*. A similar trend was observed for *2ppb Xanthan Gum + 1% KCl*, however, an increase in yield point was observed. *20%MEG + 2ppb PHPA* showed a slight decrease in PV with temperature. This fluid also showed increases in YP values after hot-rolling. The MEG/PHPA fluid superseded all other fluids in rheological properties. It also exhibited rheology which is insensitive to temperature increase.

Table 4.10: Plastic Viscosity and Yield Point Values for Improved and Special Fluids at 150˚F

	Plastic Viscosity (cp)		Yield Point ($lb/100ft^2$)	
Fluid Composition	**Before**	**After**	**Before**	**After**
2ppb PHPA + 1% KCl	7	7	14	9
2ppb Xanthan Gum + 1% KCl	7	4	16	19.5
2ppb PHPA + 20 % MEG	15	13	10	24

Table 4.11 shows the percent recoveries of the shale when exposed to the improved and special fluids at 150˚F. The MEG/PHPA system gave the highest percent recovery. This may be due to the fact that it possesses the highest apparent viscosity

enabling it to coat the shale effectively. However, the shale cuttings obtained after dispersion tests where very soft and had to be carefully handled before weighing.

The percent recoveries shown can only be used as a comparison between the fluids represented in this study. Variations in dispersion methodology, especially in sieve sizes used to recover the shale, make comparisons with other documented recoveries unfounded. However, it is expected that maximum recovery of the shales will be obtained with the use of an OBM. This has always been the case in every experiment in which WBMs are compared with OBMs.

Table 4.11: Shale Percent Recoveries for Improved and Special Fluids

Composition	% Recovery *150 °F*
2 ppb PHPA + 1% KCl	77.2
2 ppb Xanthan Gum + 1% KCl	77.3
2 ppb PHPA + 20% MEG	78.8

4.3.3 Swelling Test Results

Linear Swelling tests were carried out on the Norway and Barnett shale samples using the improved and special fluids. Table 4.12 shows the summary of the linear swelling test results. Figures 4.11and 4.12 show the semi-log plots of percent linear swelling versus time obtained for the shales when immersed in deionized water and other drilling fluids respectively. The Barnett shale did not swell in deionized water after immersion for over 5 days. Further tests were terminated due to its unreactivity. The Norway shale however showed reactivity when placed in all the test fluids. Maximum linear swell for this shale was obtained in the deionized water. Deionized water should provide the maximum swell due to its complete inability to inhibit shale swelling. The

maximum reading on the digital gauge experienced by the Norway shale was 0.0265 inches for the first trial and 0.0255 inches for the second trial. This gave a 10.6% and 10.2% linear swell respectively. A sample calculation is shown below.

Table 4.12: Linear Swelling Results

Drilling Fluid Composition	Maximum Percent Linear Swelling	Qualitative Description
De-ionized water (1)	10.6	Partial disintegration
De-ionized water (2)	10.2	Partial disintegration
2 ppb PHPA + 1% KCl	5.6	Intact, soft
2 ppb Xanthan Gum + 1% KCl	4.8	Intact, firm
2 ppb PHPA + 20% MEG	3.0	Intact, firm

$L = 0.25\ in.$

$\Delta L = 0.0265\ in.$

$$\varepsilon = \frac{\Delta L}{L} \times 100 = \frac{0.0265\ in.}{0.25\ in.} \times 100 = 10.6\%$$

where,

$L = length\ of\ shale\ slab\ (in.)$

$\Delta L = change\ in\ shale\ length\ (in.)$

$\varepsilon = percent\ linear\ swell\ (\%)$

The maximum reading on the digital gauge for *2ppb PHPA +1% KCl*, *2ppb Xanthan Gum +1% KCl*, and *20% MEG +2ppb PHPA* were 0.014 inches, 0.012 inches, and 0.0075 inches respectively. The percent linear swellings calculated from these values are 5.6%, 4.8% and 3%. All of these are lower than the value obtained for the de-ionized water. That is, they all provided inhibition to some extent. The MEG fluid superseded all

other fluids as minimum swelling was observed using this fluid while the *2ppb PHPA +1% KCl* gave the highest linear swelling.

The results obtained from swelling tests are similar to those from the dispersion tests. The MEG/PHPA fluid provided maximum inhibition for both tests. Even though swelling and dispersion are different phenomena, the *MEG/PHPA fluid* hindered them from occurring. However, the magnitude of inhibition observed in the swelling tests was higher than in the dispersion tests. Therefore, shale swelling is more sensitive to fluid selection than dispersion.

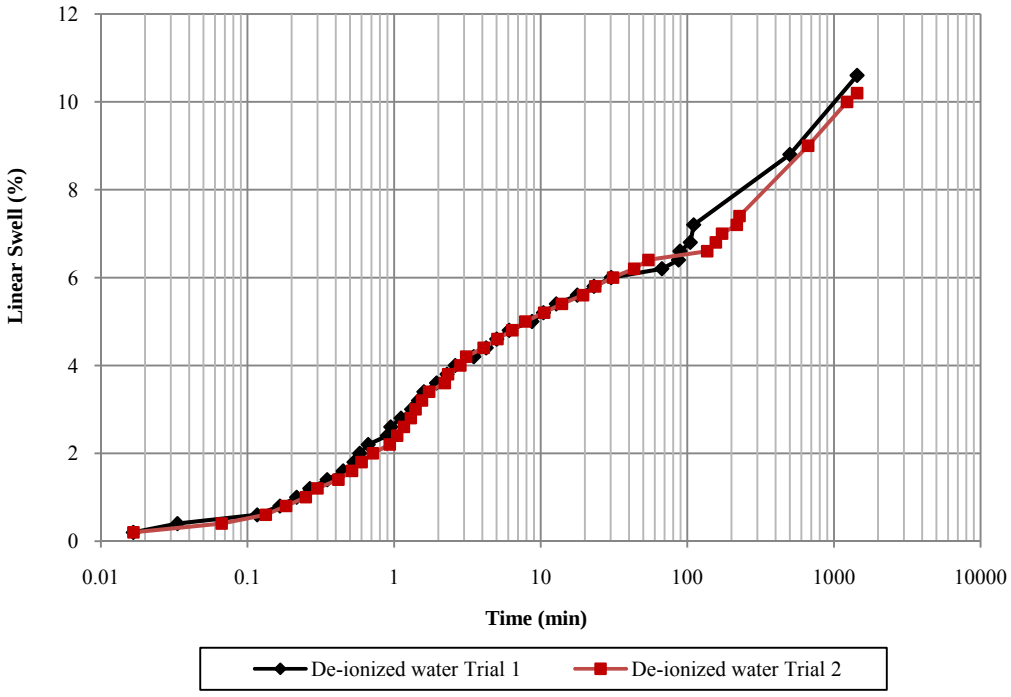

Figure 4.11: Percent Linear Swelling for Norway Shale in De-ionized water

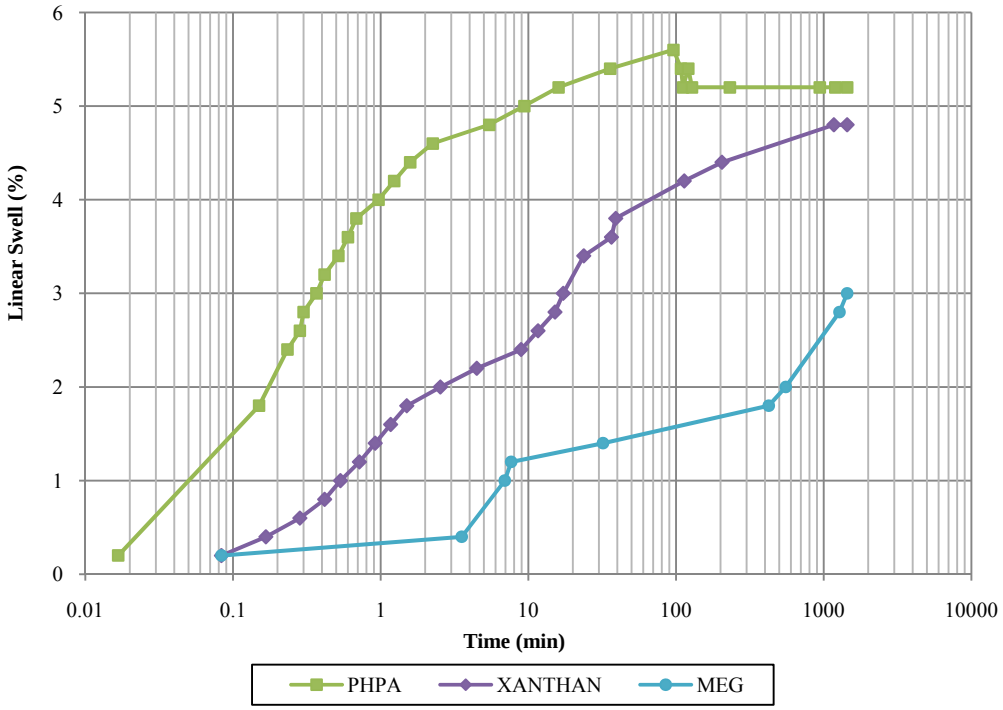

Figure 4.12: Percent Linear Swelling for Norway Shale in Improved and Special Fluid

4.4 Cost Analysis

Ultimately, drilling fluid selection is highly dependent on cost. Further evaluation on fluids based on costs is therefore essential to this study. Table 4.13 lists the respective costs of each chemical used to formulate the improved and special fluids. This was used to calculate cost per barrel of each fluid shown in Table 4.14. The MEG/PHPA fluid is the most expensive fluid at $4991.31. This is much more than the cost of the other fluids. However, the cost of methylglucoside was obtained from a scientific source and is expected to be cheaper when sold at oilfield bulk units. As the levels of inhibition obtained are not as significant, the cheaper fluids should be used. The cost of an OBM is given as $89.70 (Harris, Devon) for a typical mud used in the Arkoma Basin. This is relatively more expensive than all the water-based drilling fluids developed.

Table 4.13: Cost of Drilling Fluid Chemicals (After Mr. Harris, Devon and Fischer Scientific)

	Cost ($)	Unit (lb)	Cost/lb ($)
Potassium Chloride	120.6	50	2.41
Sodium Hydroxide	23.71	50	0.47
Bentonite	5.93	100	0.06
PHPA	81.99	43.8	1.87
Xanthan	371.52	25	14.86
MEG*	-	-	57.00

*** Price from Fischer Price**

Table 4.14: Cost of Developed Improved and Special Drilling Fluids

	Cost/bbl
2 ppb PHPA + 1% KCl	12.25
2 ppb Xanthan Gum + 1% KCl	38.23
2 ppb PHPA + 20% MEG	4991.31

CHAPTER 5: SUMMARY, CONCLUSIONS AND RECOMMENDATIONS

5.1 Summary

The objective of this study was first to characterize the Barnett and Norway shale samples obtained by determining their mineral compositions, cation exchange capacities, native moisture content and total organic content. Second, the adsorption isotherms of the shales were to be established and modeled along with existing isotherms of other shales. The final objective was to develop a water-based mud with the purpose of reducing dispersion and swelling of Norway shale.

These objectives were carried out by measuring shale properties and analyzing clay content. The adsorption isotherms of Norway, Barnett, Pierre, Wellington and Mancos shales were then modeled using the Guggenheim, Anderson and DeBoer (GAB) model. A GAB model parameter called monolayer moisture content was compared with the cation exchange capacity for each shale. Model predictions were in agreement with experimental observations.

Bentonitic and polymeric fluids composed of bentonite, partially hydrolyzed polyacrylamide (PHPA) and salt concentrations were developed and evaluated for the Norway shale using dispersion tests at ambient (75˚F), 150˚F, and 200˚F. The rheological properties of these fluids were evaluated before and after the dispersion test. Based on percent recovery values and results of rheological properties, swelling tests were executed with an improved fluid and results were compared with those obtained from other special fluids.

5.2 Conclusions

Based on the experimental results obtained from this study, the following conclusions were made.

1. Adsorption isotherms modeled for selected shales using the GAB model indicate the dependence of shale adsorptive properties on both cation exchange capacity (CEC) and total organic carbon content. Previously, only CEC was considered.
2. The Barnett shale exhibits no evidence of dispersion or swelling while the Norway shale is very reactive and will disperse and swell on exposure to aqueous fluids.
3. For the Norway shale, polymeric fluids yielded higher percent recovery values from dispersion tests than the bentonitic fluids. However, their rheological properties need to be augmented by the addition of viscosifiers before use.
4. MEG/PHPA fluid reduces dispersion greatly when compared with PHPA/salt and Xanthan/salt fluids. Hence, reduction of chemical potential by salt addition is not the only significant mechanism for developing inhibitive fluids.

5.3 Recommendations

Based on this study, the following recommendations are proposed.

1. Adsorption isotherms should be developed for shales at temperatures representative of the wellbore and temperature dependent parameters of the GAB model be analyzed.
2. Further investigation on MEG's ability to reduce shale dispersion should be carried out while exploring other uncommon oilfield materials as fluids for inhibiting shale formations.

NOMENCLATURE

a	=	activity
a_w	=	water activity
BET	=	Brunauer, Emmett and Teller
C	=	constant
C	=	Guggenheim constant
C_o	=	adjustable parameter accounting for temperature effect
$^{\circ}C$	=	degrees Celsius
CEC	=	Cation Exchange Capacity, Meq/100g Solid
$^{\circ}F$	=	degrees Fahrenheit
GAB	=	Guggenheim, Anderson, and De Boer
Δh_c	=	specific bonding enthalpy of water monolayer, J/kg
Δh_k	=	mean specific bonding enthalpy of the water multilayer, J/kg
$\Delta h_{s,\ mono}$	=	specific sorption enthalpy of water monolayer, J/kg
Δh_{vap}	=	specific vaporization enthalpy of water monolayer, J/kg
$\Delta h_{s,\ multi}$	=	mean specific sorption enthalpy of water monolayer, J/kg
K	=	Sorption energies of multiple layers of molecule
K	=	temperature dependent constant
K_o	=	adjustable parameter accounting for temperature effect
ΔL	=	change in shale length, in
L	=	original length of shale sample, in

MC	=	moisture content, %
MEG	=	methylglucoside
$meq/100gm$	=	milliequivalent weights of methylene blue per 100gm of solid
N	=	spring factor
NMC	=	native Moisture Content, %
OBM	=	Oil-Based Mud
P,p	=	pressure
p_0	=	gas saturation pressure
p/p_0	=	relative vapor pressure
P_{Π}	=	swelling pressure
P_{ads}	=	adsorptive Pressure
PHPA	=	partially hydrolyzed polyacrylamide
R	=	universal gas constant, J/kg/K
ROP	=	rate of penetration
T	=	temperature, K
TOC	=	Total Organic Content, %
V_w	=	partial molar volume of water
w_i	=	initial weight, g
w_f	=	final weight, g
W, υ	=	moisture content, kg/kg % Dry Basis
W_m, υ_m	=	monolayer moisture content, kg/kg % Dry Basis
W_c	=	weight of carbon removed by ashing, g
W_s	=	weight of shale before experimental procedure, g

W_u = weight of undispersed shale, g

W_w = weight of water removed by drying, g

W_w = weight of water gained by the shale sample, g

WBM = Water-Based Mud

XRD = X-Ray Diffraction Analysis

Greek Symbols

θ = fraction of available active sites

θ_{300} = dial reading at 300rpm

θ_{600} = dial reading at 600rpm

ε = percent linear swell, %

τ = shear stress, lbf/ft^2

τ_0 = yield stress, lbf/100ft^2

u_p = plastic viscosity, cp

γ = shear rate, 1/s

REFERENCES

1. Adamson A.W.: "Physical Chemistry of Surfaces", 4th Edition, John Wiley & Sons, pp 521-534, 1982.
2. Al-Awad N.J. and Smart B.G.D.: "Characterization of Shale-Drilling Fluid Interaction Mechanisms Related to Wellbore Instability", J. King Saud Univ., Vol.8, Eng. Sci. (2), pp 187-215, 1996.
3. Ayoub R.F., Tan C.P., Clennell B., Yang J., Tohidi, B.: "Wellbore Stability Issues in Shales or Hydrate Bearing Sediments". AAPG Hedberg Research Conference, Vancouver, September, 2004.
4. Baver L.D.: "Soil Physics", 3rd Edition, John Wiley & Sons, pp 36-37, 1956.
5. Bol G.M. *et al*.: "Borehole Stability in Shales", SPE presented at the SPE European Petroleum Conference, Cannes, November 16-18, 1992.
6. Borgoyne A.T., Chenevert M.E., Millheim K.K, Young F.S.: "Applied Drilling Engineering", SPE Textbook Series, Vol. **2**, pp 53, 76-77, 1986.
7. Boulding R. and Ginn J.S.: "Practical Handbook of Soil, Vados-Zone, and Ground-water Contamination: Assessment, Prevention, and Remediation", Edition 2, pp 5, 2003.
8. Brunauer S., Emmet P.H., Teller E.: "Adsorption of Gases in Multimolecular Layers", Journal of the American Chemical Society, Vol. **60 (2)**, pp 309-319, 1938.
9. Brunauer S.: "The Adsorption of Gases and Vapors, Princeton University Press, Princeton, 1945.
10. Bradley W.B.: "Failure of Inclined Boreholes", Journal of Energy Resources Technology Transcation of the AIME, Vol. **101,** pp 232-239, December, 1979.

11. Chenevert M.E. and Pernot V.: "Control of Shale Swelling Pressures Using Inhibitive Water Based Muds", SPE 49263 presented at the SPE Annual Technical Conference and Exhibition, New Orleans, September 27-30, 1998.
12. Chenevert, M.E. and Osisanya, S.O.: "Shale Swelling at Elevated Temperature and Pressure", presented at the 33rd Symposium in Rock Mechanics, Santa Fe, New Mexico, June 8-10, 1992.
13. Chenevert M.E.: "Shale Alteration by Water Adsorption", JPT. Vol. **22**, pp 1141-1148, 1970.
14. Chenevert M.E.: "Shale Control with Balanced Activity Oil Muds", JPT Trans AIME, Vol. **249**, pp 1309-1316, October, 1970.
15. Chenevert M.E. and Osisanya S.O.: "Shale/Mud Inhibition Defined with Rig-Site Methods", SPE Drilling Engineering, September, 1989.
16. Chunyao P., Wenqiang, Xiaolin Y., Jienian Y., Xiangdong L.: "Offshore Benign Water Drilling Fluid can Prevent Hard Brittle Shale Hydration and Maintain Borehole Stability", SPE 114649 was prepared for presentation at the IADC/SPE Asia Pacific Drilling Technology Conference and Exhibition held in Jakarta, Indonesia, August 25-27, 2008.
17. Civan F.: "Reservoir Formation Damage: Fundamentals, Modeling, Assessment, and Mitigation", pp 581, 2007.
18. Clark R.K., Scheurman R.F., Rath H., Van Larr H.G.: "Polyacrylamide/Potassium-Chloride Mud for Drilling Water-Sensitive Shales", SPE 5514, Journal of Petroleum Technology, June 7-9, 1976.

19. CRC "Hand Book of Chemistry and Physics: A Ready Reference Book of Chemistry and Physics data", 85th Edition, David R. Lide, 2004.
20. Darley H.C.H.: "A Laboratory Investigation of Borehole Stability", JPT Trans, AIME, PP 883-892**,** July, 1969.
21. Darley H.C.H and Gray G.R.: "Composition and Properties of Drilling and Completion fluids", Fifth Edition, Houston, Texas, Gulf Publishing Company, 1991.
22. Donohue M.D. and Aranovich G.L.: "Classification of Gibbs Adsorption Isotherms" Advances in Colloid and Interface Science, Vol. **76-77**, pp 137-152, 1998.
23. Dye W., Daugereau K., Hansen N., Otto M., Shoults L., Leaper R., Clapper D., Xiang T.: "New Water-Based Mud Balances High-Performance Drilling and Environmental Compliance", SPE 92367 prepared for presentation at the SPE/IADC Drilling Conference held in Amsterdam, The Netherlands, 23-25 February, 2005.
24. Ewy R.T. and Morton E.K.: "Wellbore Stability Performance of Water Based Mud Additives", SPE 116139 was prepared for presentation at the 2008 SPE Annual Technical Conference and Exhibition held in Denver, Colorado, USA, September 21-24, 2008.
25. Fellows P.: "Food Processing Technology: Principles and Practice", Edition 2, pp 46, 2000.
26. Fennema O.R.: "Food Chemistry", Second Edition, 1985.
27. Fennema O.R.: "Food Chemistry", Third Edition, pp 32, 42 and 47, 1996.
28. Figura L.O. and Teixeira A.A.: "Food Physics: Physical Properties - Measurement and Applications", pp 23-28, 2007
29. Fischer Scientific, May, 04, 2009.

http://www.fishersci.com/wps/portal/CMSTATIC?href=index.jsp&store=Scientific&segment=researchAnalytical

30. Forsans T.M., and Schmitt L.: "Capillary Forces: The Neglected Factor in Shale Instability Studies?", SPE 28029 was prepared for presentation at the Eurock SPE/ISRM Rock Mechanics in Petroleum Engineering Conference, Delft, The Netherlands, August 29-31, 1994.
31. Graber E.R. and Borisover M.: "Effect of Hydration of Organic Matter on Sorption of Organic Compounds: Data, Concept, and Sorption Isotherm Model", Geophysical Research Abstracts, Vol. **5**, 02196 © European Geophysical Society, 2003.
32. Gruszkiewicz M.S., Simonson J.M, Burchell T.D., Cole D.R.: "Water Adsorption and Desorption on Microporous Solids at Elevated Temperature", Journal of Thermal Analysis and Calorimetry, Vol. **8**, pp 609-615, 2005.
33. Guizhong C., Chenevert M.E., Sharma M.M., Yu M.: "A Study of Wellbore Stability in Shales Including Poroelsatic, Chemical, and Thermal Effects", Journal of Petroleum Science and Engineering, Vol. **38**, pp 167-176, 2003.
34. Hale A.H., Mody F.K., Salisbury D.P.: "The Influence of Chemical Potential on Wellbore Stability", SPE Drilling and Completion, pp 207-216, 1993.
35. Hale A.H.: "Experimental Investigation of the Influence of Chemical Potential on Wellbore Stability", SPE 23885 presented at the IADC/SPE Drilling Conference, New Orleans, LA, February 18-21, 1992.
36. Harris O. of Devon, Personal Communication, 2009.
37. Headley J.A, Walker T.O., Jenkins R.W.: "Environmental Safe Water-Based Drilling Fluid to Replace Oil-Based Muds for Shale Stabilization", SPE 29404 was prepared

for presentation at the SPE/IADC Drilling Conference held in Amsterdam, February 28-March 2, 1995.

38. Hiemenz P.C.: "Principles of Colloid and Surface Chemistry", Second edition, Marcel Dekker, Inc. N.Y., pp 494, 1977.
39. Hui Y.H., Barta J., Cano M.P., Gusek T.W.: "Handbook of Fruits and Fruit Processing: Science and Technology", pp 538, 2006.
40. Jenkins R.G. and Walker P.L.: "Analysis of Mineral Matter in Coal", Analytical Methods for Coal and Coal Products, Vol. 2, Karr C (ed), New York, NY, USA, Academic Press, pp 265-292, 1978.
41. Jones F.O Jr.: "New Fast, Accurate Test Measurement of Bentonite in Mud", Oil and Gas Journal, pp 76-78, June 1, 1964.
42. Kahr G. and Madsen, F.T.: "Determination of the Cation Exchange Capacity and the Surface Area of Bentonite, Illite and Kaolinite by Methylene Blue Adsorption", Applied Clay Science, Vol. **9**, pp 327-336, 1995.
43. Labuza T.P., Acott K., Tatini S.R., Lee R.Y.: "Journal of Food and Science", Vol. **41**, pp 910-917, 1976.
44. Langmuir I. Journal of American Chemical Society, Vol. 34, pp 1310, 1912.
45. Langmuir I. Journal of American Chemical Society, Vol. **40**, pp 1361, 1918.
46. Lomba R.F.T., Chenevert M.E., Sharma M.M.: "The Ion-selective Membrane Behavior of Native Shales", Journal of Petroleum Science and Engineering, Vol. **25,** pp 9-23, 2000.

47. Lomba R.F.T., Chenevert M.E., Sharma M.M.: "The Role of Osmotic Effects in Fluid Flow Through Shales", Journal of Petroleum Science and Engineering, Vol. **25**, pp 25-35, 2000.

48. Manohar L.: "Shale Stability: Drilling Fluid Interaction and Shale Strength", SPE 54356 was prepared for presentation at the SPE Latin American and Caribbean Petroleum Engineering Conference held in Caracas, Venezuela, April 21-23, 1999.

49. Masel R.I.: "Principles of Adsorption and Reaction on Solid Surfaces: Wiley Series in Chemical Engineering", 10th edition, pp 235-245, 299, 1996.

50. McMinn W.A.M. and Magee T.R.A. "Studies on the Effect of Temperature on the Moisture Sorption Characteristics of Potatoes. Journal of Food Process Engineering Vol. **22**, pp113-128, 1999.

51. Meier L.P. and Kahr G.: "Determination of the Cation Exchange Capacity (CEC) of Clay Minerals Using The Complexes of Copper (II) Ion With Triethylenetetramine and Tetraethylenepentamine", Clays and Clay Mineral, Vol. **47** (3), pp 386-388, 1999.

52. Mitchell J.K.: "Fundamentals of Soil Behavior", Wiley Interscience, Second Edition, pp 23, 28, 31, 1993.

53. MI-Swaco Drilling Fluids Engineering Manual Version 2.1. 2009.

54. Mody F.K. and Hale A.H.: "Borehole-Stability Model to Couple the Mechanics and Chemistry of Drilling-Fluid/Shale Interactions", JPT, Vol. **45**, pp 1093-1101, 1993.

55. Mondshine T.C.: "New Technique Determines Oil Mud Salinity Needs in Shale Drilling", Oil and Gas Journal, pp 70-75, July 14, 1969.

56. Mortimer G.: "Physical Chemistry", 3rd edition, pp 566-567, 2008.

57. O'Brien D.E., and Chenevert M.E.: "Stabilizing Sensitive Shales with Inhibited, Potassium-Based Drilling Fluids", JPT. Vol. **25**, pp 1089-1100, 1973.

58. Oleas A., Osuji C.E., Chenevert M.E., Sharma M.M.: "Entrance Pressure of Oil Based Mud into Shale: Effect of Shale, Water Activity, and Mud Properties", SPE 116364 was prepared for presentation at the SPE Annual Technical Conference Exhibition held in Denver, Colorado, USA, September 21-24, 2008.

59. Osisanya S.O.: "Wellsite Shale Evaluation Techniques for Control of Shale Related Wellbore Instability Problems", Masters Thesis, The University of Texas at Austin, 1986.

60. Osisanya S.O. and Chenevert M.E.: "Rigsite Shale Evaluation Techniques for Control of Shale Related Wellbore Instability Problems", SPE/IADC 16504, New Orleans, LA, March 27-April 2, 1987.

61. Osisanya S.O.: "Experimental Studies of Wellbore Stability in Shale Formations" Ph.D Dissertation, The University of Texas at Austin, 1991.

62. Osisanya S.O. and Chenevert M.E.: "Physico-Chemical Modelling of Wellbore Stability in Shale Formations", The Journal of Canadian Petroleum Technology, Vol. **35(2)**, pp 53-63, February, 1996.

63. Patel A., Stamatakis E., Young S., Friedheim J.: "Advances in Inhibitive Water-Based Drilling Fluids - Can They Replace Oil-Based Muds?", SPE 106476 prepared for presentation at the SPE International Symposium on Oilfield Chemistry held in Houston, Texas, U.S.A, 28 February-2 March, 2007.

64. Rao R.S and Leja J.: "Surface Chemistry of Froth Floatation", 2nd Edition, pp 293, 2004.

65. Resnik S.L., Favetto G., Chirife J., Fontan C.F.: "A World Survey of Water Activity of Selected Saturated Salt Solutions used as Standards at 25 ˚C", Journal of Food Science, Vol. **49**, pp 510-513, 1984.

66. Rizvi, S.S.H.: "Thermodynamic Properties of Foods in Dehydration: Engineering Properties of Foods", Edited by M.A. Rao & S.S.H. Rizvi, pp 133-214, 1986.

67. Robinson R.A. and Sinclair D.A.: "The Activity Coefficient of Alkali Chlorides and of Lithium Iodide in Aqueous Solution from Vapor Pressure Measurements", J. Phy. Chem., Vol. **56**, pp 1830-1832, September, 1934.

68. Rosco Moss Company: "Handbook of Groundwater Development", pp 160, 1990.

69. Russell J.M.: "Interaction of Slaughterhouse Effluent Protein with Three New Zealand Soils", N.A. Journal of Agricultural Research, Vol. **25**, pp 24, 1982.

70. Santos H., Diek A., Roegiers J-C., Fontoura S.A.B.: "Investigation of the Effects of Sample Handling Procedures on Shale Properties", Rock Mechanics, Balkema, 1996.

71. Santos H.M.R.: "A New Conceptual Approach to Shale Stability", Ph.D Dissertation, The University of Oklahoma, Norman, Oklahoma, pp 39, 1997.

72. Schechter R.S.: "Oil Well Stimulation", pp 33-39, 1990.

73. Schlumberger Oilfield Glossary. http://www.glossary.oilfield.slb.com

74. Sherwood J.D.: "Ionic Transport in Swelling Shale", Advances in Colloid and Interface Science, Vol. **61**, pp 51- 64, 1995.

75. Simpson J.P., Walker T.O., Jiang G.Z.: "Environmentally Acceptable Water Based Muds can Prevent Shale Hydration and Maintain Wellbore Stability", SPE 27496 was first presented at the IADC/SPE Drilling Conference held in Dallas, Texas, February 15-18, 1995.

76. Singh P.C. and Singh R.K.: "Application of GAB Model for Water Sorption Isotherms of Food Products", Journal of Food Processing and Preservation, Vol. **20** pp 203-220, 1996.

77. Staverman A.J.: "Non Equilibrium Thermodynamics of Membrane Processes", Trans. Faraday Soc., Vol. **48**, pp 176, 1952.

78. Steiger R.P. and Leung P.K.: "Quantitative Determination of Mechanical Properties of Shales", SPE Drilling Engineering, pp 181, 1992.

79. Sun Drilling Products Corporation, "The Hole Solution Company". 2009. http://www.sundrilling.com/images/balled%20bit%20JPG%20web.JPG

80. Tan K.H.: "Principles of Soil Chemistry", pp 451, 1998.

81. Tsiapouris A. and Linke L.: "Water Vapor Sorption Determination of Starch Based Porous Packaging Materials", Starch, Vol. **52 (2-3)**, pp 53-57, 2000.

82. Udy P.B.: "Factors Influencing the Release of Insecticides from Granular Formulations and their Subsequent Diffusion into a Range of New Zealand Soils", N.A. Journal of Agricultural Research, Vol. **20**, pp 83, 1976.

83. Van Den Berg C. and Bruin S.: "Water activity and its estimation in food systems: theoretical aspects, In Water Activity: Influence on Food Quality" (L.B. Rockland and G.E. Stewart, eds) Academic Press New York, pp 45, 1981.

84. Van O.E., Hale A.H., Mody F.K., and Roy S.: "Transport in Shales and the Design of Improved Water-Based Drilling Fluids", SPE 28309, Drilling and Completion, pp 137-146, September, 1996.

85. Van O.H.: "Compaction of Clay Sediments in the Range of Molecular Particle Distances", Clays Clay Miner, Vol. **11**, pp 178-187, 1963.

86. Wang Y. and Padua G.W.: “Water Sorption of Extruding Zein Films”, Journal of Agricultural and Food Chemistry, Vol. **52**, pp 3100-3105, 2004.
87. Wikipedia. The Free Encyclopedia. Wikipedia.com
88. Yariv S., Nasser A., Bar-on, P.: “Metachromasy in Clay Minerals”, Journal of the Chemical Society, Faraday Transactions, Vol: **86**, 1593, 1990.
89. Yu M., Chen G., Chenevert M.E., Sharma M.M.: “Chemical and Thermal Effects on Wellbore Stability of Shale Formations”, SPE 71366 was prepared for presentation at the SPE Annual Technical Conference and Exhibition held in New Orleans, Louisiana, 30 September-3 October, 2001.
90. Yu X.: “Investigation of Moisture Sorption Properties of Food Materials Using Saturated Salt Solution and Humidity Generating Techniques, PhD Dissertation, The University of Illinois at the Urbana-Champaign, 2007.

APPENDIX A – DATA SPREADSHEETS

Table A. 1: Adsorption Isotherms

	NORWAY			BARNETT		
Water Activity	**$Weight_{Initial}$ (g)**	**$Weight_{Final}$ (g)**	**% Difference**	**$Weight_{Initial}$ (g)**	**$Weight_{Final}$ (g)**	**% Difference**
0	0.0000	0.0000	0.0000	0.0000	0.0000	0.0000
0.11	5.0023	5.0317	0.5877	5.0019	5.0074	0.1098
0.30	5.0027	5.0883	1.7111	5.0038	5.0134	0.1915
0.51	5.0026	5.2418	4.7815	5.0023	5.0173	0.2990
0.76	5.0051	5.4931	9.7501	5.0041	5.0293	0.5011
0.86	5.0051	5.6227	14.5361	5.0015	5.0329	0.6239
0.96	5.0040	6.1041	21.9844	5.0006	5.0418	0.8172

Table A. 2: Adsorption Isotherm Modeling for Wellington and Pierre Shales

	WELLINGTON			PIERRE	
Wm	1.031			1.547	
C	3.882			4.294	
K	0.7851			0.8102	
R^2 value	0.996			0.984	
Aqueous Activity	**Experimental Data**	**Model Data**	**Aqueous Activity**	**Experimental Data**	**Model Data**
0	0	0	0	0	0
0.10	0.3132	0.3494	0.10	1.0915	0.6048
0.29	1.2796	1.1577	0.29	1.7832	1.9450
0.50	1.7342	1.9016	0.50	2.8517	3.1082
0.75	2.7426	2.7116	0.75	4.8962	4.4122
0.92	3.7166	3.6340	0.92	5.5880	6.1047
0.96	3.9496	3.9994	0.96	6.6795	6.7681
			0.98	7.5173	7.2437

Table A. 3: Adsorption Isotherm Modeling for Mancos Shale

		MANCOS	
Wm		0.3554	
C		6.992	
K		0.8692	
R^2 value		0.998	
Aqueous Activity	**Aqueous Activity**	**Experimental Data**	**Model Data**
0	0	0	0
0.10	0.10	0.265	0.2429
0.29	0.29	0.662	0.6693
0.50	0.50	0.884	0.9202
0.75	0.75	1.291	1.2456
0.92	0.92	1.800	1.8671
0.96	0.96	2.200	2.1652

Table A. 4: Adsorption Isotherm Modeling for Barnett and Norway Shales

	NORWAY		BARNETT	
Wm	4.568		0.1701	
C	1.017		3.442	
K	0.8672		0.8328	
R^2 value	0.998		0.996	
Aqueous Activity	**Experimental Data**	**Model Data**	**Experimental Data**	**Model Data**
0	0	0	0	0
0.11	0.5877	0.5352	0.1098	0.0626
0.30	1.7111	1.9941	0.1915	0.1934
0.51	4.7815	4.5995	0.2990	0.3243
0.76	9.7501	10.3889	0.5011	0.4945
0.86	14.5361	15.0353	0.6239	0.6147
0.96	21.9844	23.5560	0.8172	0.8213

Table A. 5: Total Organic Content

% TOC Norway	6.1					
% TOC Barnett	2.9					
	Crucible (g)	**Crucible + Sample Before (g)**	**Sample Before (g)**	**Crucible + Sample After (g)**	**Sample After (g)**	**%TOC**
Norway 1	12.6229	12.7355	0.1126	12.729	0.0065	5.8
Norway 2	12.0665	12.1728	0.1063	12.166	0.0068	6.4
Barnett 1	11.2242	11.3601	0.1359	11.356	0.0041	3.0
Barnett 2	12.0674	12.2110	0.1436	12.207	0.0040	2.8

Table A. 6: Barnett Shale Native Moisture Content

Barnett					
Trials	**1**	**2**	**3**	**4**	**Average**
$Weight_{Initial}$	7.9252	6.9644	6.4976	8.3772	
$Weight_{24\ hrs}$	7.9024	6.9440	6.4779	8.3480	
% Native Moisture	0.29	0.29	0.30	0.35	0.3

Table A. 7: Norway Shale Native Moisture Content

Norway					
Trials	**1**	**2**	**3**	**4**	**Average**
$Weight_{Initial}$	4.3950	3.2715	4.4230	4.7318	
$Weight_{24\ hrs}$	3.6084	2.6342	3.5899	3.8174	
% Native Moisture	17.90	19.48	18.84	19.32	18.9

Cation Exchange Capacity

$$CEC = \frac{C_D \times V_{MB} \times C_{MB}}{V_{DF} \times M_S}$$

$C_D = 3500$

$C_{MB} = 0.01$

$V_{DF} = 2ml$

$M_S = 10g$

$V_{MBnorway} = 5.5ml$

$V_{MBbarnett} = 2.5ml$

Table A. 8: Percent Linear Swell for Norway Shale in Deionized Water

Length (in)	0.25	DEIONIZED WATER					
NorwayTrial 1				Norway Trial 2			
Time (s)	Time (min)	Gauge Reading (in)	% Linear Swell	Time (s)	Time (min)	Gauge Reading (in)	% Linear Swell
0	0	0	0	0	0.00	0	0
1	0.02	0.0005	0.2	1	0.02	0.0005	0.2
2	0.03	0.001	0.4	4	0.07	0.001	0.4
7	0.12	0.0015	0.6	8	0.13	0.0015	0.6
10	0.17	0.002	0.8	11	0.18	0.002	0.8
13	0.22	0.0025	1	15	0.25	0.0025	1
16	0.27	0.003	1.2	18	0.30	0.003	1.2
21	0.35	0.0035	1.4	25	0.42	0.0035	1.4
27	0.45	0.004	1.6	31	0.52	0.004	1.6
32	0.53	0.0045	1.8	36	0.60	0.0045	1.8
35	0.58	0.005	2	43	0.72	0.005	2
40	0.67	0.0055	2.2	56	0.93	0.0055	2.2
54	0.90	0.006	2.4	63	1.05	0.006	2.4
57	0.95	0.0065	2.6	70	1.17	0.0065	2.6
67	1.12	0.007	2.8	78	1.30	0.007	2.8
79	1.32	0.0075	3	84	1.40	0.0075	3
88	1.47	0.008	3.2	93	1.55	0.008	3.2
96	1.60	0.0085	3.4	104	1.73	0.0085	3.4
117	1.95	0.009	3.6	133	2.22	0.009	3.6
138	2.30	0.0095	3.8	140	2.33	0.0095	3.8
157	2.62	0.01	4	170	2.83	0.01	4
210	3.50	0.0105	4.2	186	3.10	0.0105	4.2
255	4.25	0.011	4.4	245	4.08	0.011	4.4
301	5.02	0.0115	4.6	304	5.07	0.0115	4.6
366	6.10	0.012	4.8	384	6.40	0.012	4.8
524	8.73	0.0125	5	471	7.85	0.0125	5
627	10.45	0.013	5.2	633	10.55	0.013	5.2
767	12.78	0.0135	5.4	837	13.95	0.0135	5.4
1067	17.78	0.014	5.6	1167	19.45	0.014	5.6
1387	23.12	0.0145	5.8	1411	23.52	0.0145	5.8
1817	30.28	0.015	6	1868	31.13	0.015	6
4029	67.15	0.0155	6.2	2604	43.40	0.0155	6.2
5233	87.22	0.016	6.4	3257	54.28	0.016	6.4
5350	89.17	0.0165	6.6	8194	136.57	0.0165	6.6
6291	104.85	0.017	6.8	9385	156.42	0.017	6.8
6637	110.62	0.018	7.2	10364	172.73	0.0175	7
30031	500.52	0.022	8.8	13047	217.45	0.018	7.2
86400	1440.00	0.0265	10.6	13620	227.00	0.0185	7.4
				40027	667.12	0.0225	9
				73675	1227.92	0.025	10
				86400	1440.00	0.0255	10.2

Table A. 9: Percent Linear Swell for Norway Shale in PHPA and Xanthan Fluids

Length (in)	0.25						
PHPA				XANTHAN			
Time (s)	Time (min)	Gauge Reading (in)	% Linear Swell	Time (s)	Time (min)	Gauge Reading (in)	% Linear Swell
0	0	0	0	0	0	0	0
1	0.02	0.0005	0.2	5	0.08	0.0005	0.2
9	0.15	0.0045	1.8	10	0.17	0.001	0.4
14	0.23	0.006	2.4	17	0.28	0.0015	0.6
17	0.28	0.0065	2.6	25	0.42	0.002	0.8
18	0.30	0.007	2.8	32	0.53	0.0025	1
22	0.37	0.0075	3	43	0.72	0.003	1.2
25	0.42	0.008	3.2	55	0.92	0.0035	1.4
31	0.52	0.0085	3.4	70	1.17	0.004	1.6
36	0.60	0.009	3.6	90	1.50	0.0045	1.8
41	0.68	0.0095	3.8	152	2.53	0.005	2
58	0.97	0.01	4	268	4.47	0.0055	2.2
74	1.23	0.0105	4.2	535	8.92	0.006	2.4
95	1.58	0.011	4.4	697	11.62	0.0065	2.6
135	2.25	0.0115	4.6	908	15.13	0.007	2.8
326	5.43	0.012	4.8	1033	17.22	0.0075	3
563	9.38	0.0125	5	1422	23.70	0.0085	3.4
960	16.00	0.013	5.2	2190	36.50	0.009	3.6
2146	35.77	0.0135	5.4	2340	39.00	0.0095	3.8
5760	96.00	0.014	5.6	6815	113.58	0.0105	4.2
6480	108.00	0.0135	5.4	12274	204.57	0.011	4.4
6687	111.45	0.013	5.2	70253	1170.88	0.012	4.8
7257	120.95	0.0135	5.4	86400	1440.00	0.012	4.8
7690	128.17	0.013	5.2				
13867	231.12	0.013	5.2				
56378	939.63	0.013	5.2				
71763	1196.05	0.013	5.2				
86400	1440.00	0.013	5.2				

Table A. 10: Percent Linear Swell for Norway Shale in MEG fluid

Length (in)	0.25		
MEG			
Time (s)	Time (min)	Gauge Reading (in)	% Linear Swell
0	0	0	0
5	0.08	0.0005	0.2
212	3.53	0.0010	0.4
415	6.92	0.0025	1.0
458	7.63	0.0030	1.2
1920	32.00	0.0035	1.4
25455	424.25	0.0045	1.8
33168	552.80	0.0050	2.0
76563	1276.05	0.0070	2.8
86400	1440.00	0.0075	3.0

APPENDIX B – RHEOGRAMS

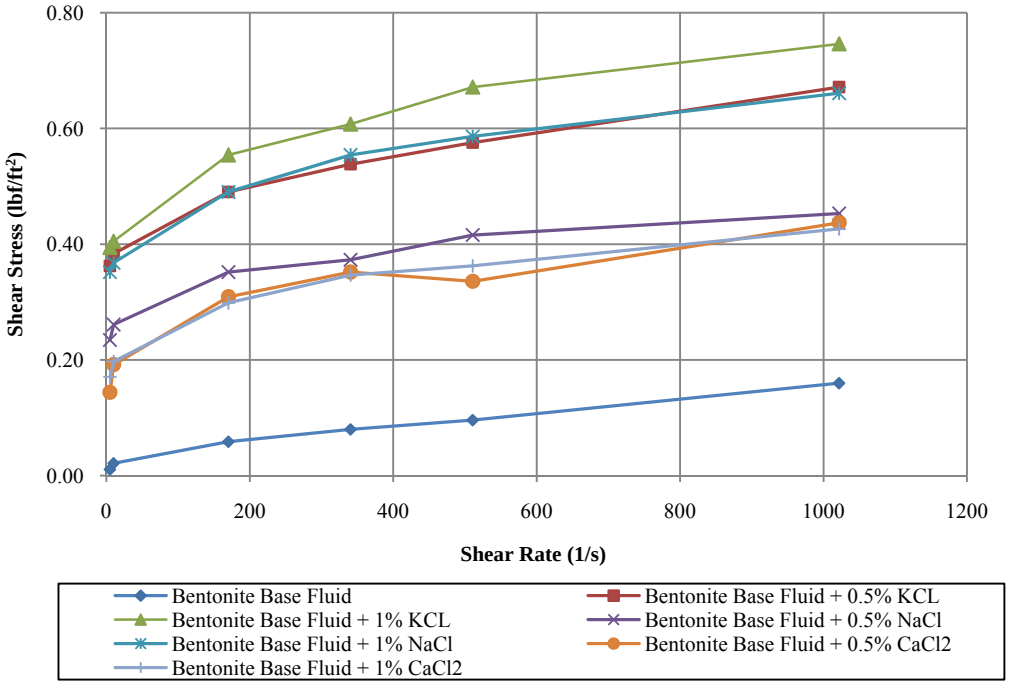

Figure B. 1: Rheogram for Bentonitic Fluids before Dispersion Tests at 75˚F

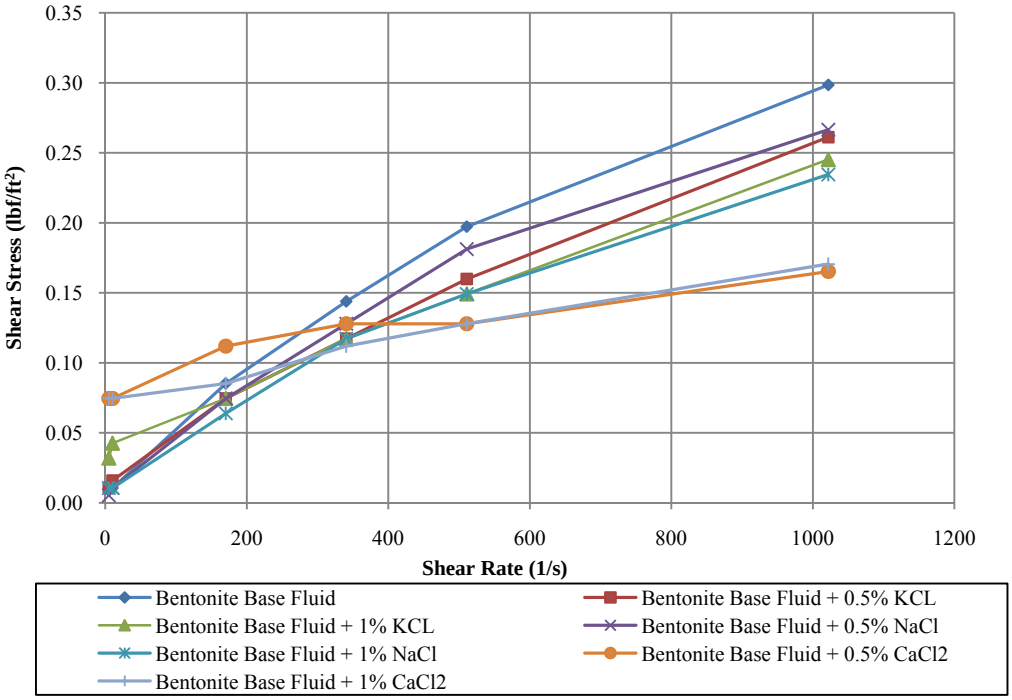

Figure B. 2: Rheogram for Bentonitic Fluids after Dispersion Tests at 75˚F

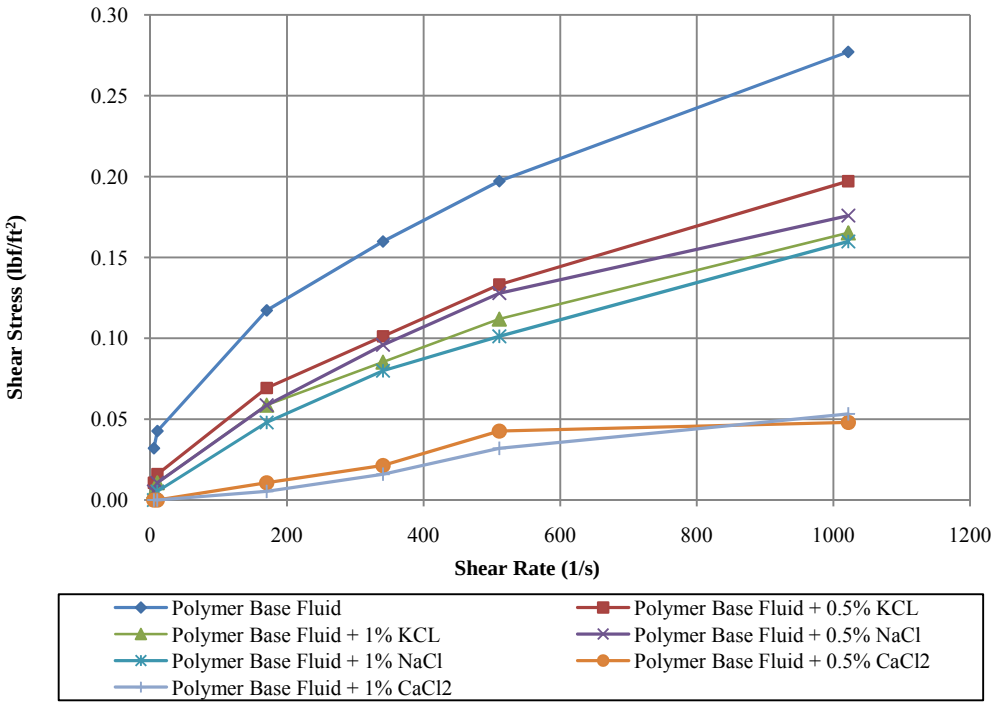

Figure B. 3: Rheogram for Polymeric Fluids before Dispersion Tests at 75˚F

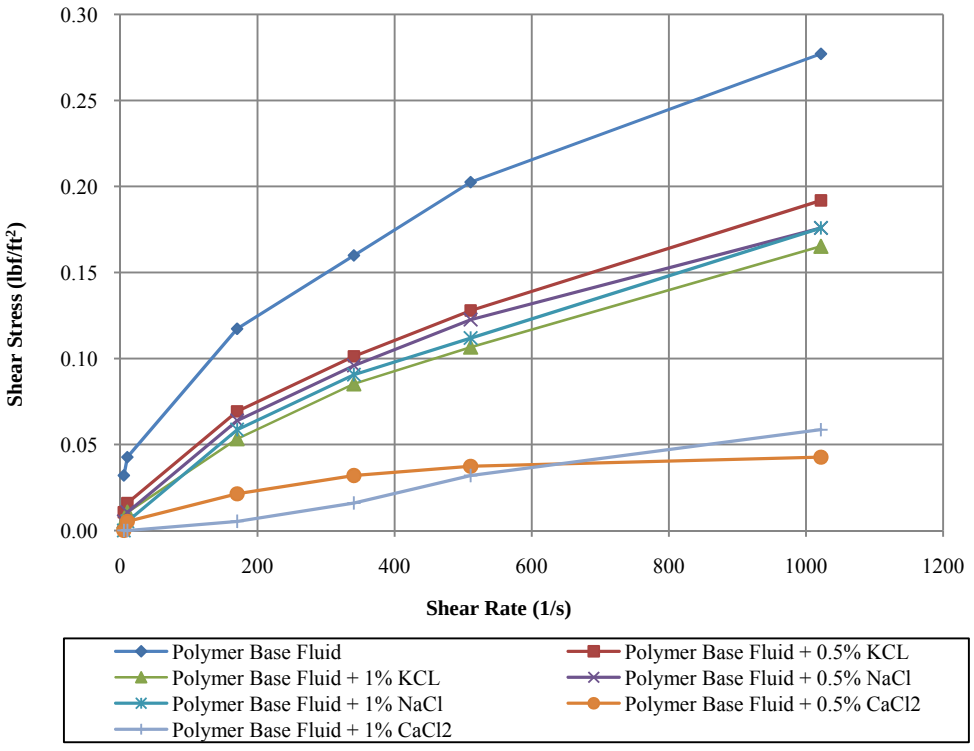

Figure B. 4: Rheogram for Polymeric Fluids after Dispersion Tests at 75˚F

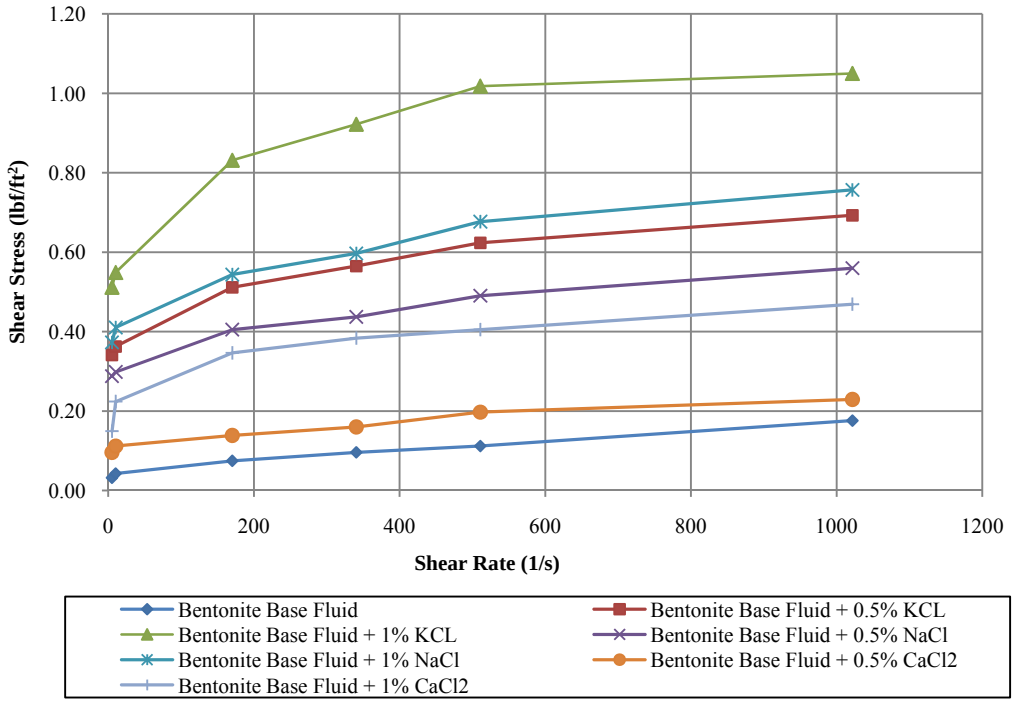

Figure B. 5: Rheogram for Bentonitic Fluids before Dispersion Tests at 150˚F

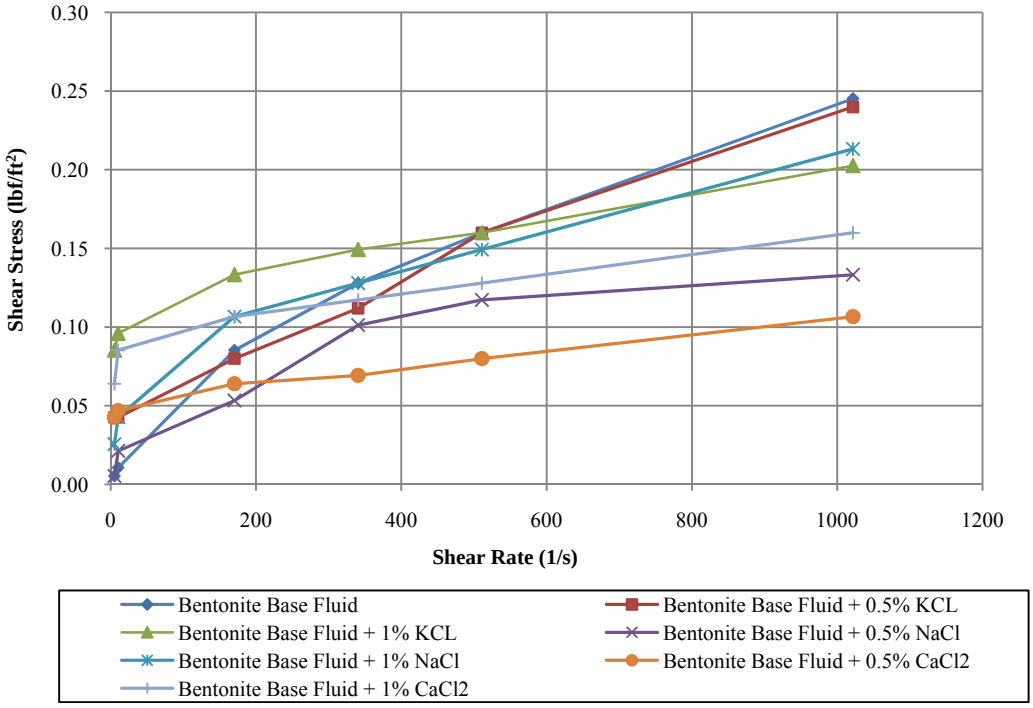

Figure B. 6: Rheogram for Bentonitic Fluids after Dispersion Tests at 150˚F

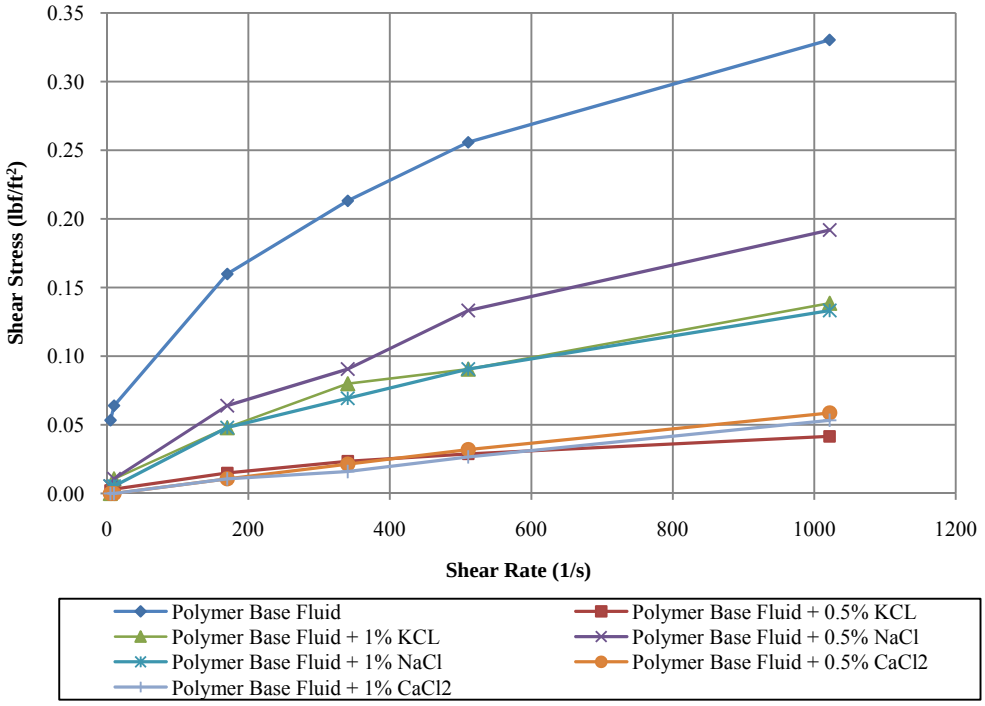

Figure B. 7: Rheogram for Polymeric Fluids before Dispersion Tests at 150˚F

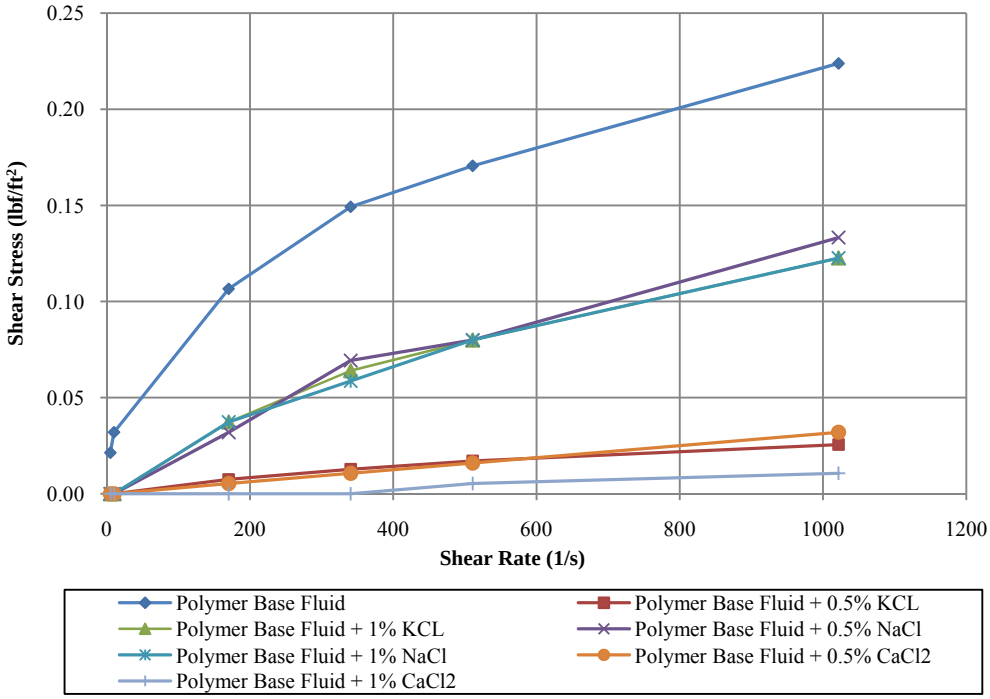

Figure B. 7: Rheogram for Polymeric Fluids after Dispersion Tests at 150˚F

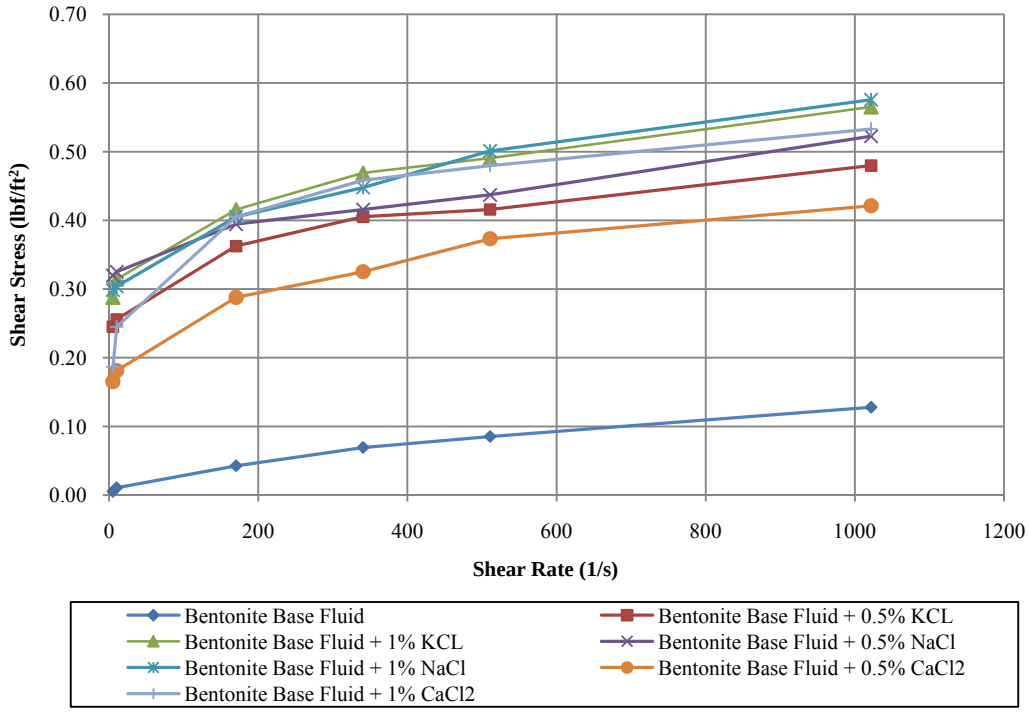

Figure B. 8: Rheogram for Bentonitic Fluids before Dispersion Tests at 200˚F

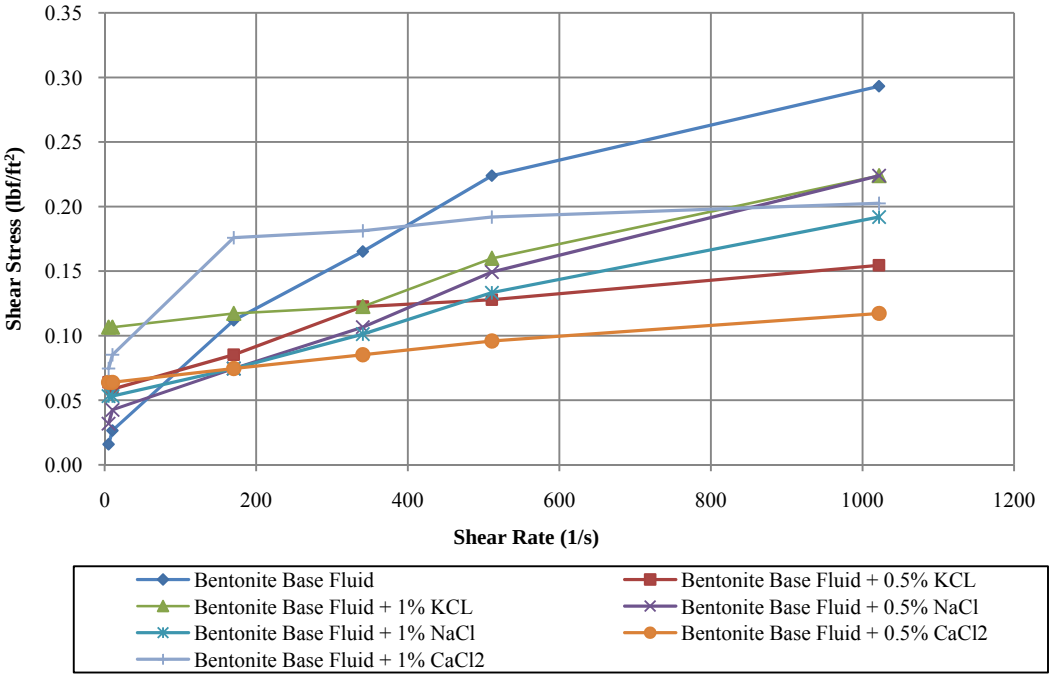

Figure B. 9: Rheogram for Bentonitic Fluids after Dispersion Tests at 200˚F

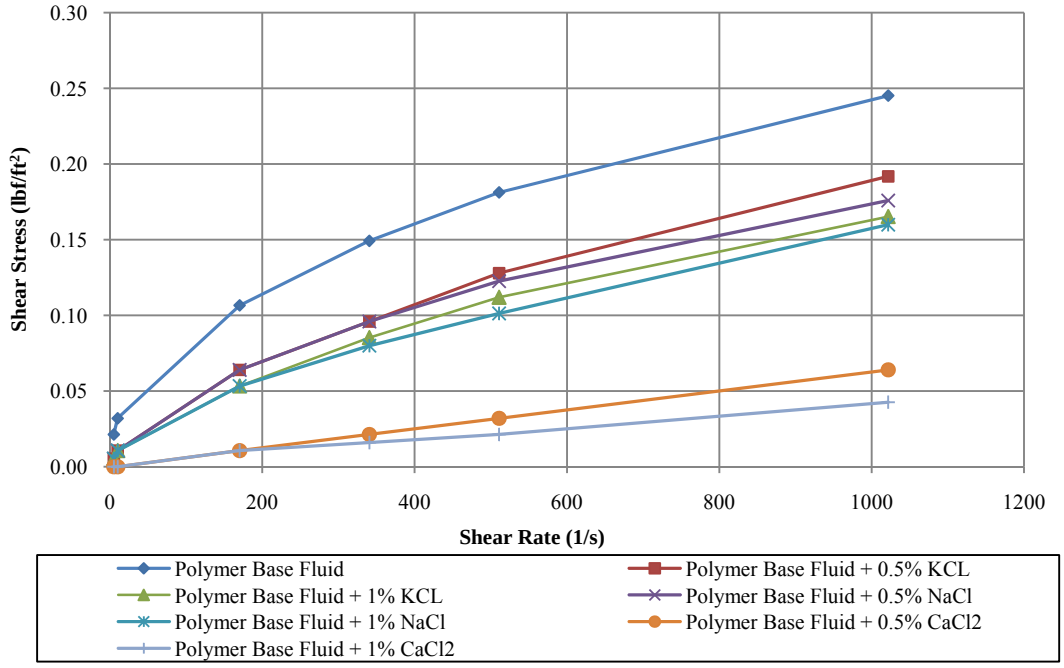

Figure B. 10: Rheogram for Polymeric Fluids before Dispersion Tests at 200˚F

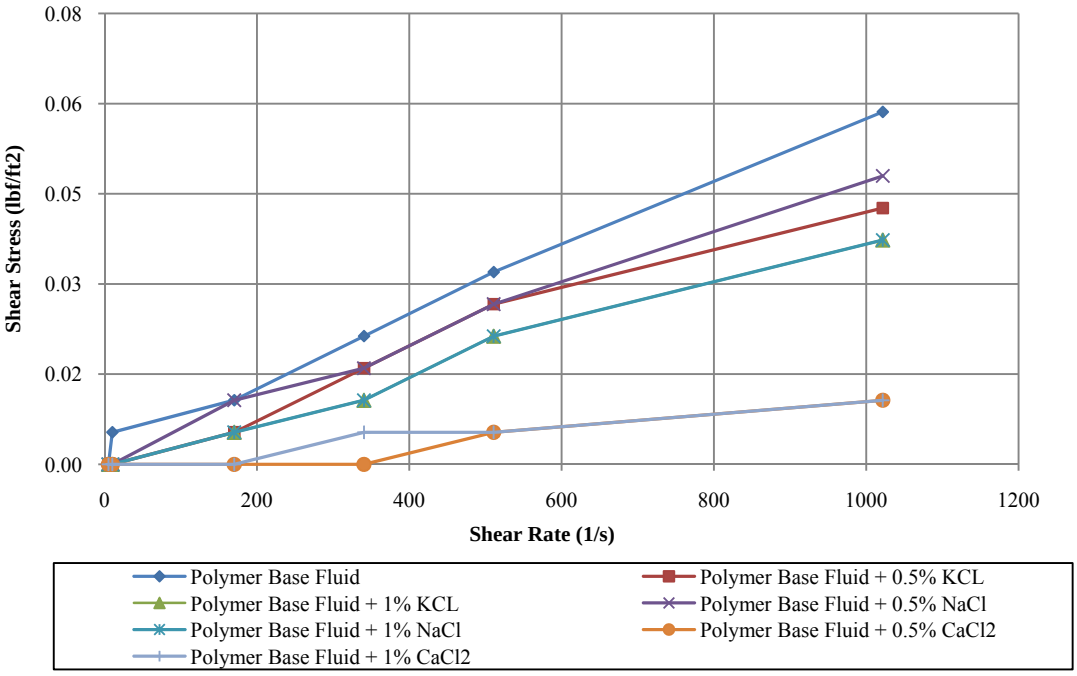

Figure B. 11: Rheogram for Polymeric Fluids after Dispersion Tests at 200˚F